T216149

NAVAL POSTGRADUATE SCHOOL
Monterey, California

THESIS

HEAT TRANSFER MEASUREMENTS OF
INTERNALLY FINNED ROTATING HEAT PIPES

by

Adnan Nefesoglu

December 1983

Thesis Advisor: P. J. Marto

Approved for public release; distribution unlimited.

REPORT DOCUMENTATION PAGE

READ INSTRUCTIONS BEFORE COMPLETING FORM

1. REPORT NUMBER
2. GOVT ACCESSION NO.
3. RECIPIENT'S CATALOG NUMBER

4. TITLE (and Subtitle)
Heat Transfer Measurements of Internally Finned Rotating Heat Pipes

5. TYPE OF REPORT & PERIOD COVERED
Master's Thesis
December 1983

6. PERFORMING ORG. REPORT NUMBER

7. AUTHOR(s)
Adnan Nefesoglu

8. CONTRACT OR GRANT NUMBER(s)

9. PERFORMING ORGANIZATION NAME AND ADDRESS
Naval Postgraduate School
Monterey, California 93943

10. PROGRAM ELEMENT, PROJECT, TASK AREA & WORK UNIT NUMBERS

11. CONTROLLING OFFICE NAME AND ADDRESS
Naval Postgraduate School
Monterey, California 93943

12. REPORT DATE
December 1983

13. NUMBER OF PAGES
102

14. MONITORING AGENCY NAME & ADDRESS(if different from Controlling Office)

15. SECURITY CLASS. (of this report)
Unclassified

15a. DECLASSIFICATION/DOWNGRADING SCHEDULE

16. DISTRIBUTION STATEMENT (of this Report)
Approved for public release; distribution unlimited.

17. DISTRIBUTION STATEMENT (of the abstract entered in Block 20, if different from Report)

18. SUPPLEMENTARY NOTES

19. KEY WORDS (Continue on reverse side if necessary and identify by block number)
Condenser, Enhancement, Condensation, Noncondensable Gases, Rotating Heat Pipe, Performance, Helical and Straight Fin, Internal Heat Transfer Coefficient.

20. ABSTRACT (Continue on reverse side if necessary and identify by block number)
A rotating cylindrical heat pipe was tested using various internally finned condensers and was compared with a smooth-wall cylinder. Each condenser was tested at rotational speeds of 700, 1400 and 2800 rpm with film condensation. Distilled water was used as the working fluid.

The heat transfer rate of each condenser was plotted versus the driving temperature difference between the vapor saturation

temperature and the cooling water inlet temperature. The objective of this investigation was to study the performance with various fin configurations and to find an optimum fin geometry.

As expected, in all cases, performance was improved with increasing rpm. The performance of internally finned condensers was found to be as much as 230 percent greater than that of the smooth condenser.

Approved for public release; distribution unlimited.

Heat Transfer Measurements of Internally Finned Rotating Heat Pipes

by

Adnan Nefesoglu
Lieutenant J. G., Turkish Navy
Turkish Naval Academy, 1976

Submitted in partial fulfillment of the
requirements for the degree of

MASTER OF SCIENCE IN MECHANICAL ENGINEERING

from the

NAVAL POSTGRADUATE SCHOOL
December 1983

DUDLEY KNOX LIBRARY

ABSTRACT

A rotating cylindrical heat pipe was tested using various internally finned condensers and was compared with a smooth-wall cylinder. Each condenser was tested at rotational speeds of 700, 1400 and 2800 rpm with film condensation. Distilled water was used as the working fluid.

The heat transfer rate of each condenser was plotted versus the driving temperature difference between the vapor saturation temperature and the cooling water inlet temperature. The objective of this investigation was to study the performance with various fin configurations and to find an optimum fin geometry.

As expected, in all cases, performance was improved with increasing rpm. The performance of internally finned condensers was found to be as much as 230 percent greater than that of the smooth condenser.

TABLE OF CONTENTS

I. INTRODUCTION 13

A. THE ROTATING HEAT PIPE 13

B. BACKGROUND 13

C. THESIS OBJECTIVES 16

II. EXPERIMENTAL EQUIPMENT 18

A. DESCRIPTION OF EQUIPMENT 18

B. INSTRUMENTATION 30

III. EXPERIMENTAL PROCEDURES 35

A. INSTALLATION AND TESTS 35

B. PREPARATION OF THE HEAT PIPE INTERIOR . . . 36

C. FILLING PROCEDURE 37

D. VENTING PROCEDURE 37

E. RUNNING PROCEDURE 38

F. DATA REDUCTION 39

IV. PRESENTATION AND DISCUSSION OF RESULTS 42

A. GENERAL COMMENTS 42

B. RESULTS OF SMOOTH WALL CONDENSER 42

C. RESULTS OF STRAIGHT 22 FIN CONDENSER 51

D. RESULTS OF HELICAL 14 AND 16 FIN CONDENSER . 51

E. RESULTS OF HELICAL 36 FIN CONDENSER 53

F. INTERNAL HEAT TRANSFER ENHANCEMENT 57

V. CONCLUSIONS AND RECOMMENDATIONS 65

A. CONCLUSIONS 65

B. RECOMMENDATIONS 66

APPENDIX A. UNCERTAINTY ANALYSIS 67

APPENDIX B. CALIBRATION 71

APPENDIX C. DATA ANALYSIS PROGRAM AND TABULATED RESULTS 79

LIST OF REFERENCES 99

INITIAL DISTRIBUTION LIST 101

LIST OF TABLES

1.1 SPECIFICATIONS OF THE INTERNALLY FINNED TUBES . . 29

C.1 RESULTS OF SMOOTH WALL CONDENSER AT 700 RPM . . . 84

C.2 RESULTS OF SMOOTH WALL CONDENSER AT 1400 RPM . . 85

C.3 RESULTS OF SMOOTH WALL CONDENSER AT 2800 RPM . . 86

C.4 RESULTS OF STRAIGHT 22 FIN CONDENSER AT 700 RPM . 87

C.5 RESULTS OF STRAIGHT 22 FIN CONDENSER AT 1400 RPM 88

C.6 RESULTS OF STRAIGHT 22 FIN CONDENSER AT 2800 RPM 89

C.7 RESULTS OF HELICAL 16 FIN CONDENSER AT 700 RPM . 90

C.8 RESULTS OF HELICAL 16 FIN CONDENSER AT 1600 RPM . 91

C.9 RESULTS OF HELICAL 16 FIN CONDENSER AT 2800 RPM . 92

C.10 RESULTS OF HELICAL 14 FIN CONDENSER AT 700 RPM . 93

C.11 RESULTS OF HELICAL 14 FIN CONDENSER AT 1600 RPM 94

C.12 RESULTS OF HELICAL 14 FIN CONDENSER AT 2800 RPM 95

C.13 RESULTS OF HELICAL 36 FIN CONDENSER AT 700 RPM . 96

C.14 RESULTS OF HELICAL 36 FIN CONDENSER AT 1400 RPM 97

C.15 RESULTS OF HELICAL 36 FIN CONDENSER AT 2800 RPM 98

LIST OF FIGURES

1.1 THE ROTATING HEAT PIPE 14

2.1 PHOTOGRAPH OF THE ROTATING HEAT PIPE SYSTEM. . . . 19

2.2 CROSS-SECTIONAL DRAWING OF THE ROTATING HEAT PIPE. 20

2.3 SCHEMATIC DIAGRAM OF THE ROTATING HEAT PIPE SYSTEM 22

2.4 PHOTOGRAPH OF A SECTION OF THE STRAIGHT 22 FIN CONDENSER. 25

2.5 PHOTOGRAPH OF A SECTION OF THE HEICAL 16 FIN CONDENSER. 26

2.6 PHOTOGRAPH OF A SECTION OF THE HELICAL 14 FIN CONDENSER. 27

2.7 PHOTOGRAPH OF A SECTION OF THE HELICAL 36 FIN CONDENSER. 28

2.8 VACUUM AND PRESSURE TEST SYSTEM. 31

2.9 THERMOCOUPLE LOCATIONS 33

4.1 SMOOTH CONDENSER THERMAL PERFORMANCE 43

4.2 SHERWOOD NUMBER VS. NUSSELT NUMBER FOR CONSTANT WALL TEMPERATURE 47

4.3 SHERWOOD NUMBER VS. NUSSELT NUMBER FOR CONSTANT WALL HEAT FLUX 48

4.4 WALL TEMPERATURE DISTRIBUTION OF SMOOTH-WALL CONDENSER AT 90 DEGREE C SATURATION TEMPERATURE. . 50

4.5 STRAIGHT 22-FIN CONDENSER THERMAL PERFORMANCE . . 52

4.6 HELICAL 16-FIN CONDENSER THERMAL PERFORMANCE . . . 54

4.7 HELICAL 14-FIN CONDENSER THERMAL PERFORMANCE . . . 55

4.8 HELICAL 36-FIN CONDENSER THERMAL PERFORMANCE . . . 56

4.9 INTERNAL ENHANCEMENT OF STRAIGHT FINNED CONDENSER 60

4.10 INTERNAL ENHANCEMENT OF HELICAL 16-FIN CONDENSER 61

4.11 INTERNAL ENHANCEMENT OF HELICAL 14-FIN CONDENSER 62

4.12 INTERNAL ENHANCEMENT OF HELICAL 36-FIN CONDENSER 63

4.13 VARIATION OF FILM THICKNESS WITH RPM 64

B.1 COOLING WATER INLET TEMPERATURE THERMOCOUPLE CALIBRATION CURVE 73

B.2 COOLING WATER OUTLET TEMPERATURE THERMOCOUPLE CALIBRATION CURVE 74

B.3 HELICAL 16-FIN CONDENSER WALL THERMOCOUPLES CALIBRATION CURVE 76

B.4 HELICAL 14-FIN CONDENSER CALIBRATION 77

B.5 HELICAL 36-FIN CONDENSER CALIBRATION 78

NOMENCLATURE

A_i	inner surface area, m^2
C_p	specific heat, kJ/kgK
D_o	outside diameter, m
g	acceleration of gravity ($\omega^2 r$), m/s^2
h_f	finned condenser internal heat-transfer coefficient, $W/m^2.K$
h_{fg}	latent heat of vaporization, kJ/kg
h_i	internal heat-transfer coefficient, $W/m^2.K$
h_o	external heat-transfer coefficient, $W/m^2.K$
h_s	smooth condenser internal heat transfer coefficient, $W/m^2.K$
k	thermal conducivity, W/m.K
k_w	wall thermal conductivity, W/m.K
L	Length, m
$\dot{m}$	mass flow rate of coolant kg/s
Q	heat-transfer rate from the condensing Vapor, W
Q_f	frictional heat rate, W
Q_t	the total heat-transfer rate from the cooling water, W
r_i	inner radius, m
r_o	outer radius, m

T_{ci} cooling water inlet temperature, Degrees C

T_{co} cooling water outlet temperature, Degrees C

T_f film temperature, Degrees C

T_{wi} inside wall temperature, Degrees C

T_{wo} outside wall temperature, Degrees C

ΔT temperature difference, $T_s - Tw_i$, Degrees C

M dynamic viscosity, kg/m.S

ω angular velocity, rad/s

ρ density of condensate, kg/m^3

σ surface tension, N/m.

ACKNOWLEDGMENT

The author wishes to express his appreciation to his advisor, Professor P. J. Marto, for his advice, support and patient guidance throughout the project.

My sincere appreciation to Dr. A. S. Wanniarachchi, for his expertise in the area and for his tireless efforts during the course of this effort.

Special thanks to Mr. Thomas Christian, Mr. Willard Dames, and Mr. John Moulton for their technical assistance.

I. INTRODUCTION

A. THE ROTATING HEAT PIPE

The rotating heat pipe is a device to transfer heat from a rotating heat source. This device basically consists of a cylindrical evaporator and condenser and a working fluid to transfer energy from one end to other (Figure 1.1).

During operation the heat pipe is rotated and the working fluid makes an annular shape in the evaporator section. Heat supplied to the evaporator vaporizes a portion of the working fluid, creating a pressure gradient from the evaporator to the opposite end.

To remove heat from the condenser, external cooling is applied to the condenser and the working fluid vapor condenses on the inner wall. Condensate flows back to the evaporator by the driving force of the pressure gradient resulting from the axial difference in the condensate film thickness along the condenser wall.

B. BACKGROUND

The first rotating heat pipe at the Naval Postgraduate School was designed and constructed by Daley [Ref. 1] in 1970. He used stainless steel for his truncated-cone condenser with a three-degree half angle. In 1971, Newton [Ref. 2] performed experiments with the basic

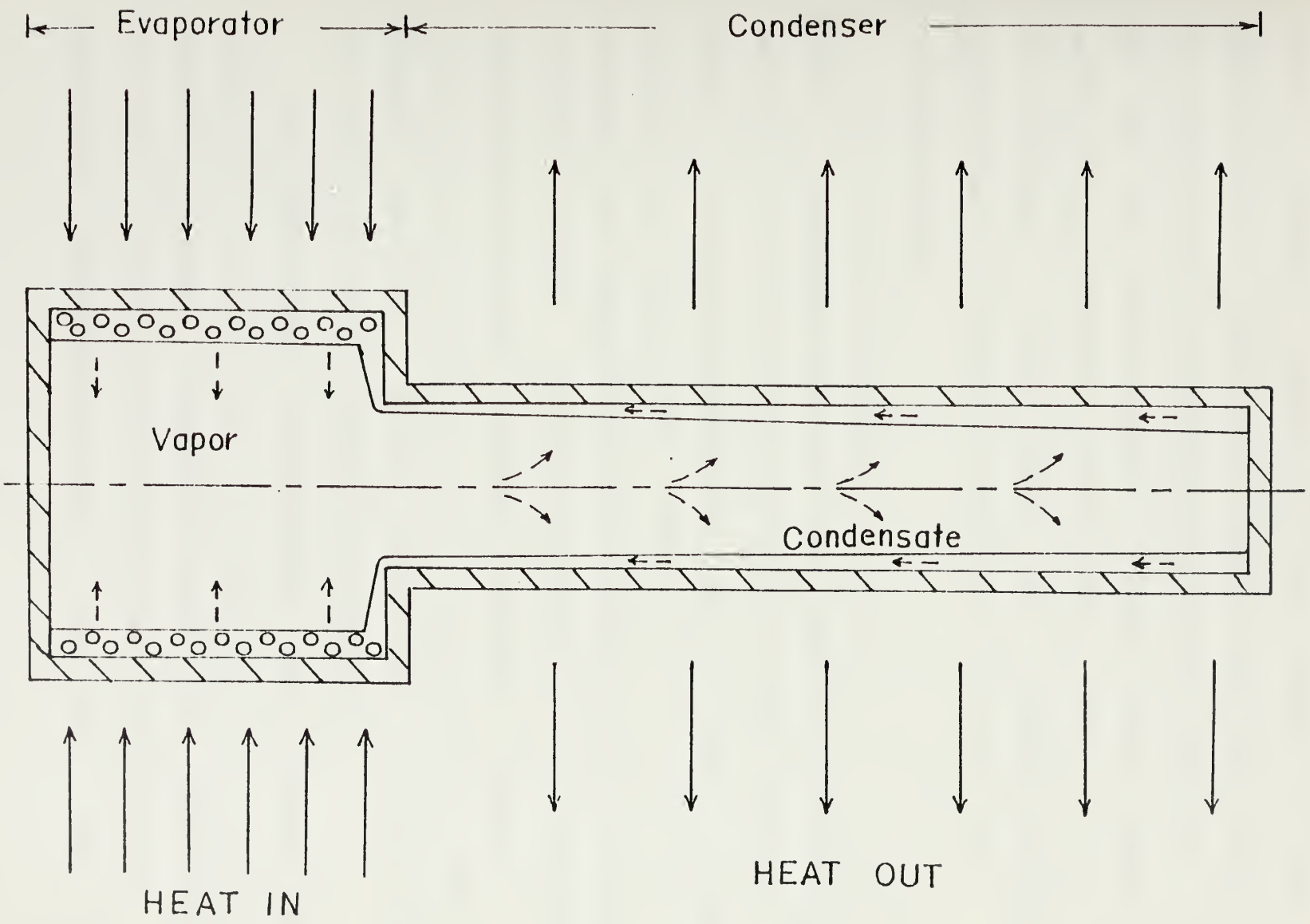

Figure 1.1 The Rotating Heat Pipe

system from Daley, using distilled water as the working fluid at rotational speeds of 700 and 1400 rpm. In 1972, Woodard [Ref. 3] continued by using the same basic system and the same working fluid at 700, 1400 and 2800 rpm. In the same year, Schaffer [Ref. 4] tested truncated copper condensers with different working fluids (alcohol, freon 113 and water). In 1974, Tucker [Ref. 5] examined dropwise condensation by coating the condenser inner wall with a silicone grease.

With all the system problems known up to 1976, Loynes [Ref. 6] redesigned the system parts and ran the experiment and obtained results similar to those of Tucker [Ref. 5]. Later in the same year, Wagenseil [Ref. 7] tested the same truncated cone with filmwise condensation. Further, he examined both smooth-walled and internally-finned cylindrical condenser sections. In 1977, Tantrakul [Ref. 8] obtained experimental data for 0.5-degree-cone-angle, truncated, cylindrical condensers with various working fluids (water, ethanol, freon 113). In 1979, Weigel [Ref. 9] tested smooth and internally-finned cylindrical condensers.

Four years later in 1983, Gardner [Ref. 10] brought the system back into operation. His objective was to examine various cylindrical, internally-finned tubes. His attempts to take data were somewhat discouraging because of the presence of noncondensable gases in the system. Also, he

had problems with the thin (0.12-mm dia.) thermocouple wires he used and with the pin connectors. The small size of the wires and the rectangular shape of the connector caused detachment of the thermocouple wires at high rotational speeds because of the large centrifugal forces.

C. THESIS OBJECTIVES

Gardner [Ref. 10] recommended that the following modifications be made on the apparatus:

1. Fix vacuum leaks to avoid any in-leaks of noncondensable gas (air) into the system during operation.
2. Design a new, cylindrical strip terminal to replace the pin connectors to allow wall thermocouple calibration in a calibration bath and protect wires from breaking away at high rotational speeds.
3. Design a new cooling water mixing chamber for good mixing of water to minimize fluctuations of the cooling water outlet temperature.

Following the above-mentioned modifications, the primary objectives of this thesis were:

1. To produce experimental results for a smooth cylindrical pipe and compare with Wagenseil's data for one-inch-diameter smooth pipe. In addition to this comparison, these data are used to provide a basis for the evaluation of various internally-finned pipes.

2. To use commercially-available, cylindrical, condensers which are internally finned (both straight and helical fins) to find the optimum fin geometry (i.e., fin density, helix angle, and relative fin size such as fin height/condenser diameter).

II. EXPERIMENTAL EQUIPMENT

A. DESCRIPTION OF EQUIPMENT

The experimental apparatus is shown in Figure 2.1. Figure 2.2 shows a cross-sectional view of the heat pipe, while Figure 2.3 shows a schematic of the apparatus. The entire system is bolted to a steel bed-plate which can be oriented from horizontal to a near-vertical position.

1. Evaporator

The evaporator (Figure 2.1) is a copper cylinder with o-ring seals at each end. The dimensions are 100mm in diameter and 70mm in length.

2. Heater

The heater (Figure 2.1) is a chromel - a wire with magnesium oxide insulation in an inconel sheath. Savereisen insulation is placed over the heater followed by a quilted insulating pad taped around the heater, and wrapped around with 6mm-wide, woven, nylon tape. This thermal insulation was secured in three places by wires. Electrical power to the rotating heater is supplied through four pairs of carbon brushes riding on a pair of bronze collector rings. The resistance of heater is 1.8 ohms at the collector rings.

3. Power Supply

A single-phase, 440-volt, 60-Hz line voltage, regulated by a voltage sensing circuit, was used to

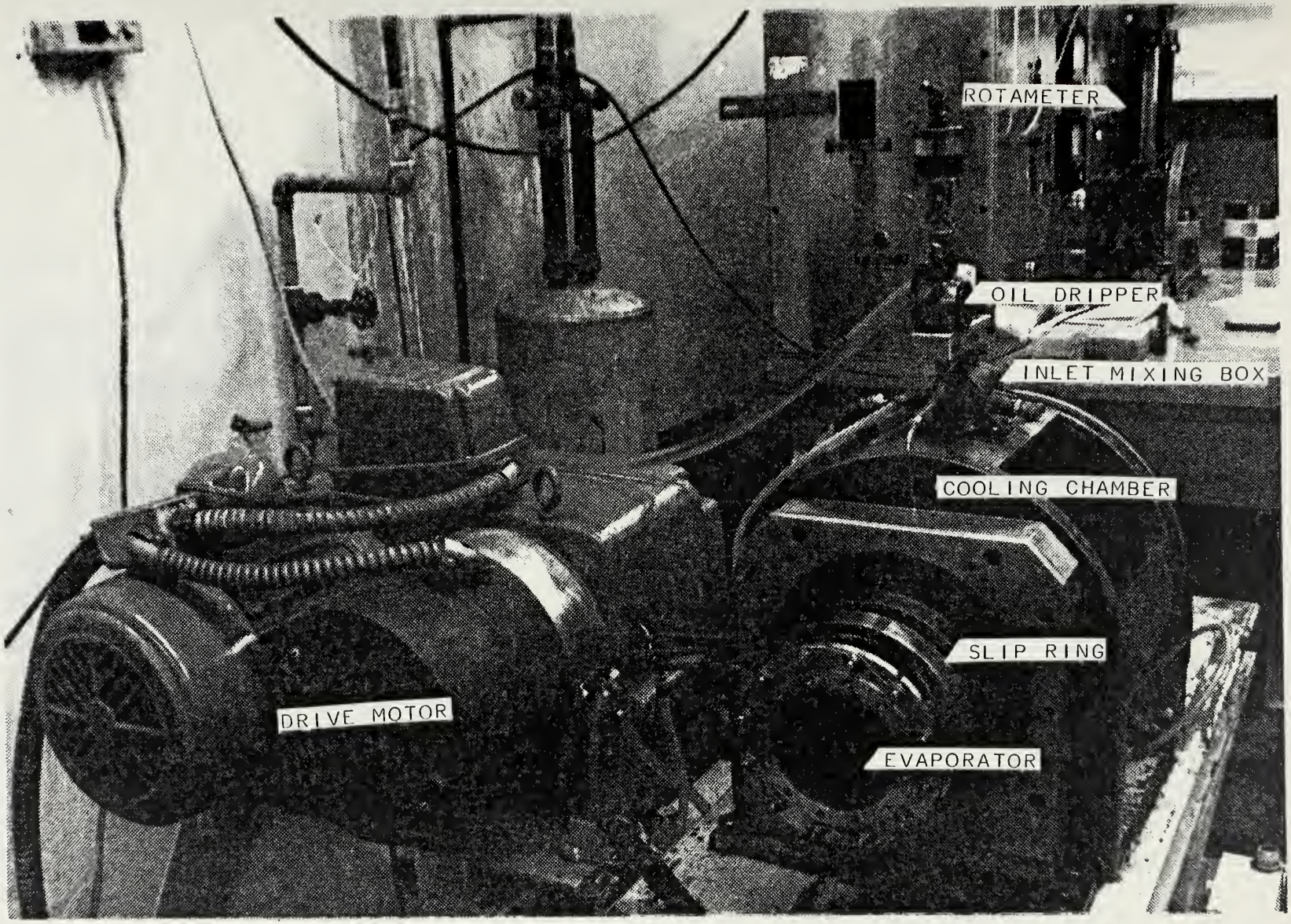

Figure 2.1 Photograph of the Rotating Heat Pipe System

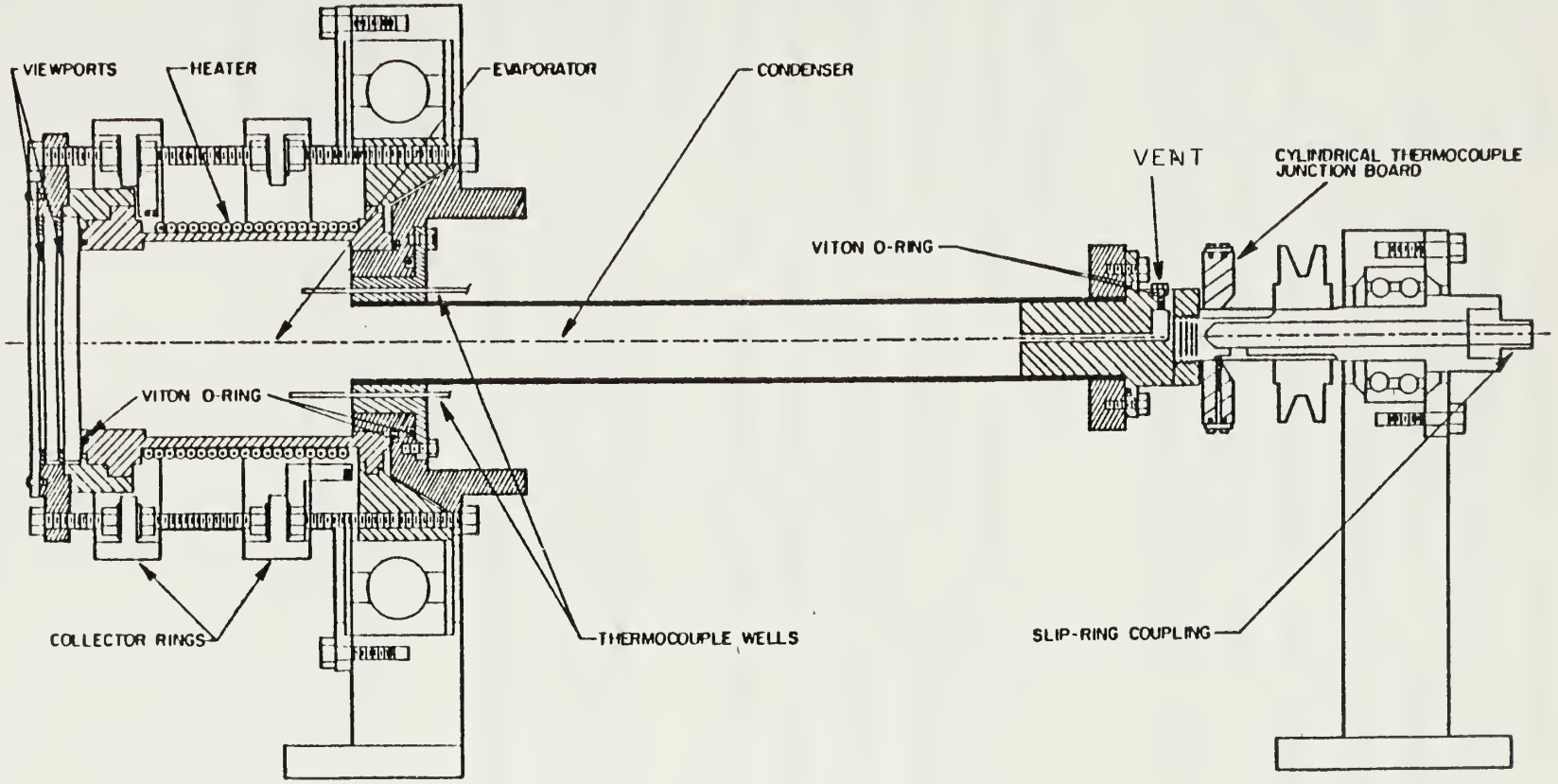

Figure 2.2 Cross-Sectional Drawing of the Rotating Heat Pipe

provide power to the heater. This line voltage was fed into a differential voltage attenuator that divided it by one hundred. This divided voltage then passed through a true-mean-square (TRMS) converter with an integration period of 1ms. The output of TRMS converter was controlled by a potentiometer on the control panel. The comparator output was fed to the control input of a Holmar silicon rectifier, which supplied amplified voltage to the collector rings.

4. View Windows

Two 88.9mm diameter, 6.35mm-thick, pyrex glass windows were mounted on the evaporator. The two glasses were separated by 2mm by placing two gaskets between them. The air gap between the two glasses minimized fogging on the inner glass for easy observation during operation.

5. Bearings

The heat pipe was supported by two bearings. The main bearing was externally cooled by water, and was lubricated by an oil dripper. The drive-pulley bearing was a self-lubricated, sealed bearing.

During the process of this work, the mounting of the main bearing was unchanged, and Gardner's [Ref. 10] method was used.

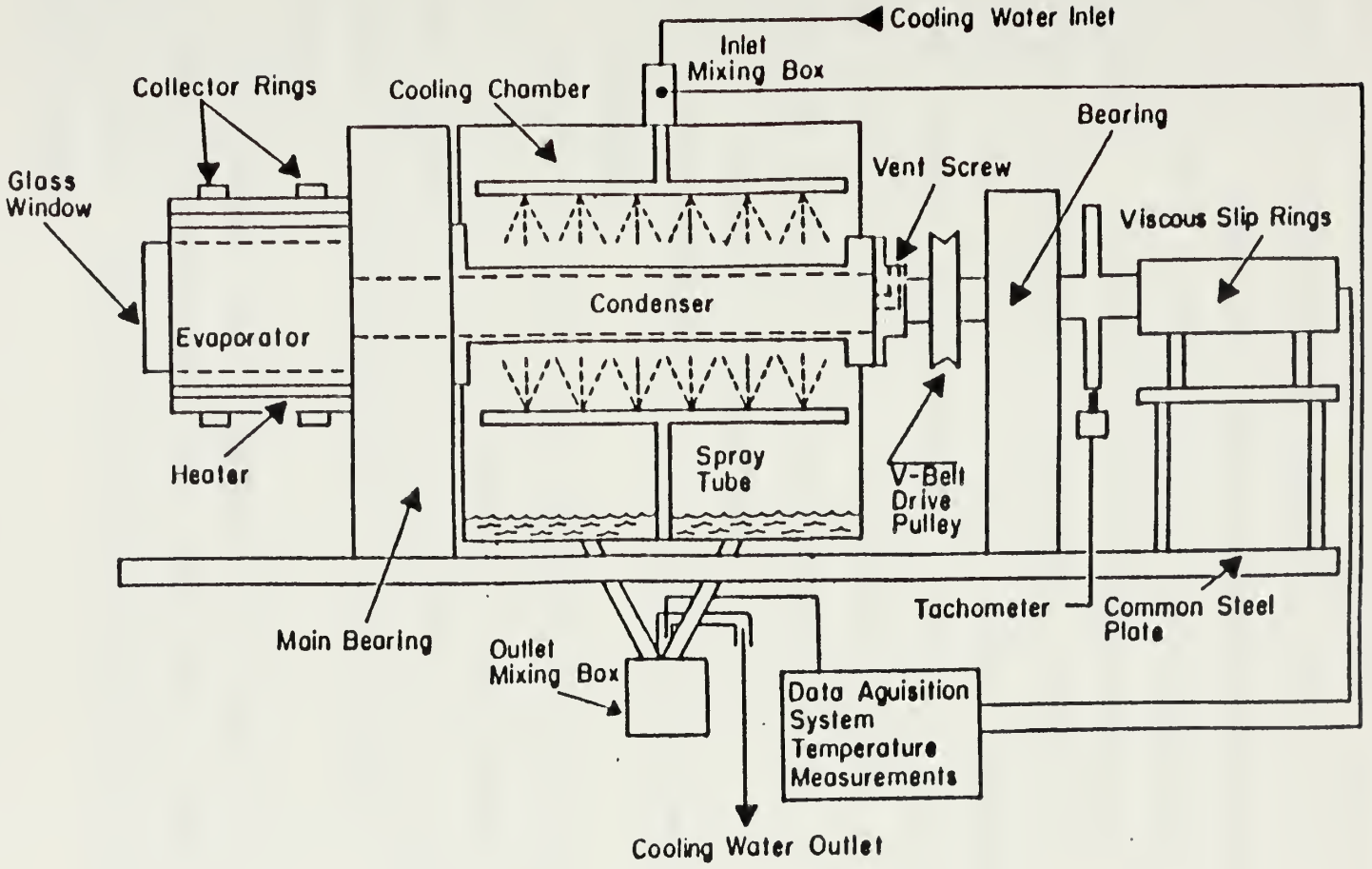

Figure 2.3 Schematic Diagram of the Rotating Heat Pipe System

6. Cooling System

As shown in Figure 2.3, the condenser was cooled by a spray of filtered-and-softened tap water. Cooling water sprayed along the condenser from four tubes placed at 90 degrees apart around the condenser. Sprayed water drained through two holes at the bottom of the cooling box into the mixing chamber. The cooling water temperatures were read by a single thermocouple at the inlet, and by five parallel thermocouples at the mixing-chamber outlet, respectively. Since the previous mixing chamber caused large temperature variations (up to $\pm$ 1.1 K), a new mixing chamber was designed (see Figure 2.3). This chamber provided more acceptable temperature fluctuations ($\pm$ 0.2 K). The cooling water flow rate was measured by a calibrated rotameter.

7. Condenser

During this work, the condensers built by Gardner [Ref. 10] were used. As an important modification, the drive-end flange was rebuilt as recommended by Gardner to eliminate one of the improperly placed o-rings (Figure 2.2).

Five copper test condensers were tested for this thesis. Each condenser was 295mm long with an effective length of 250mm. Spray cooling was provided only over the effective length.

As a basis for all different inside geometries, a smooth pipe was used with the following dimensions:

outer diameter : 26.6mm

inner diameter : 22.9mm

These pipe dimensions are the same as that used by Wagenseil [Ref. 7] and Gardner [Ref. 10] for their comparison purposes.

The other four finned condensers contained either straight or helical fins which were provided by Noranda Metal Industries of Newton, Connecticut.

1. Straight 22-fin condenser (Figure 2.4).
2. Helical 16-fin condenser which was tested by Weigel [Ref. 9] (Figure 2.5).
3. Helical 14-fin condenser (Figure 2.6).
4. Helical 36-fin condenser (Figure 2.6).

Specifications of these internally finned condensers are listed in Table (2.1).

8. System Drive and RPM Counter

The heat pipe was rotated by a variable-speed electric motor. A v-belt provided between the motor pulley and the pulley on the heat-pipe axis drove the system. Rotational speed was measured by a digital frequency counter attached to the system through a gear. Speed controller it had an accuracy of $\pm$ 1 rpm.

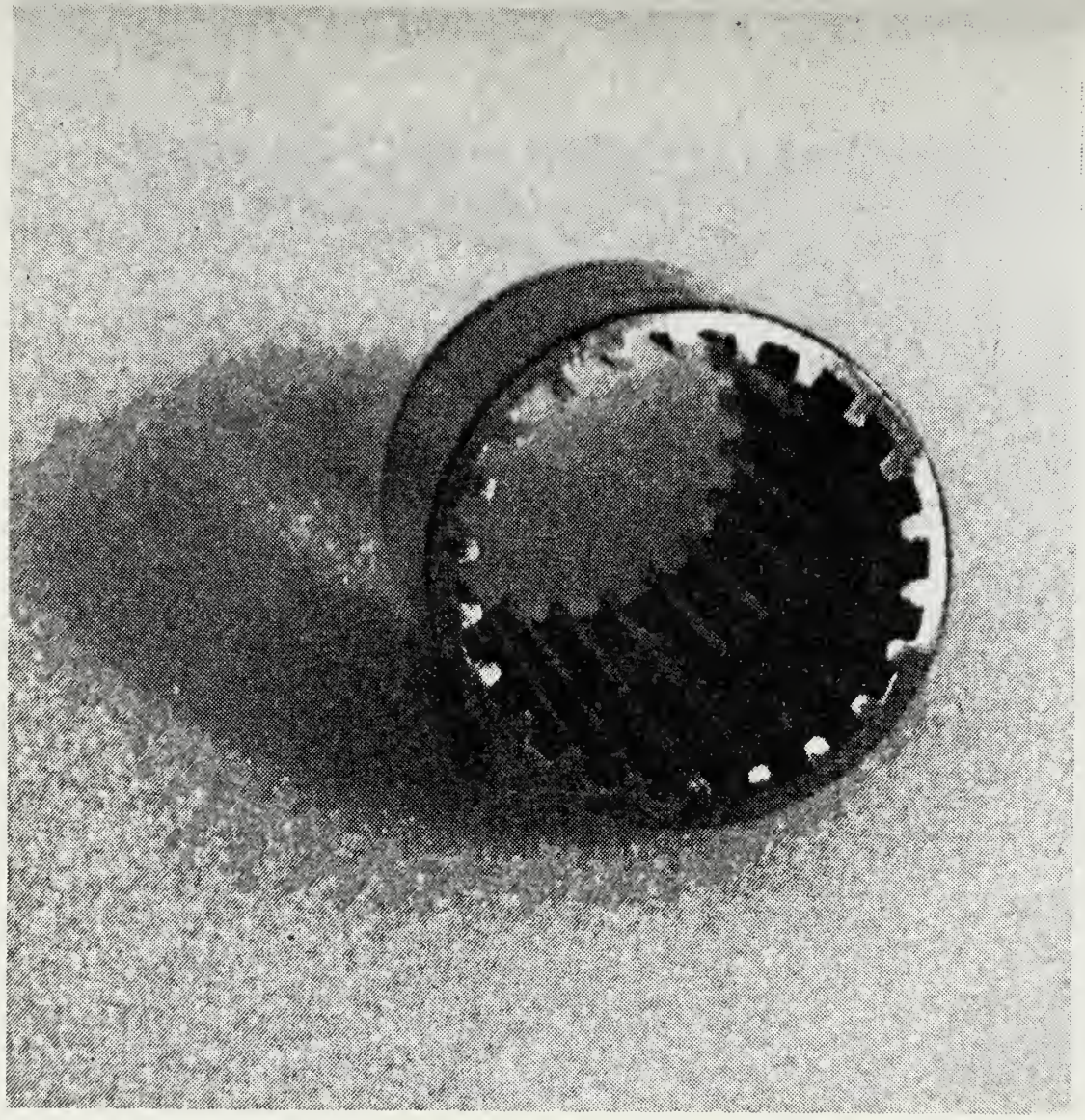

Figure 2.4 Photograph of a Section of the 22 Straight Fin Condenser

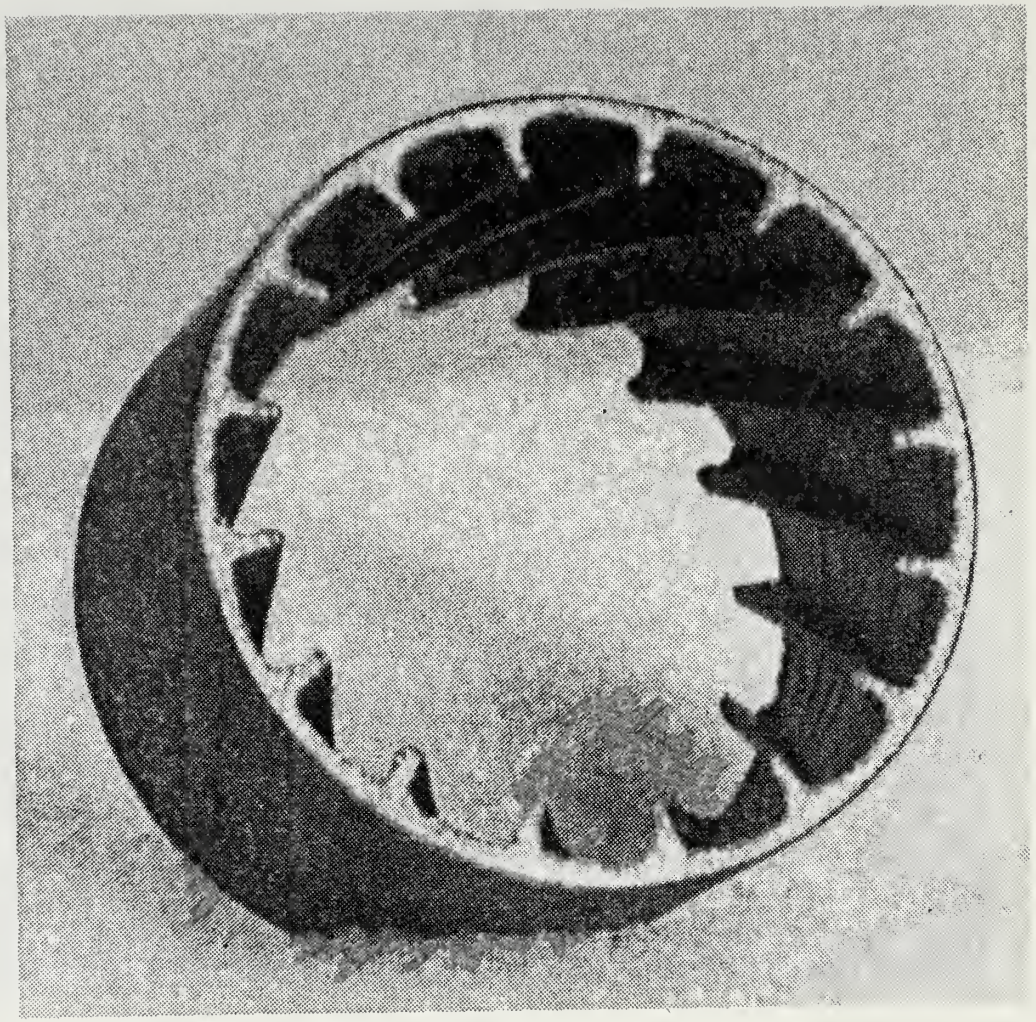

Figure 2-5 Photograph of a Section of the Helical 16-Fin Condenser.

Figure 2.6 Photograph of a Section of the Helical 14 Fin Condenser

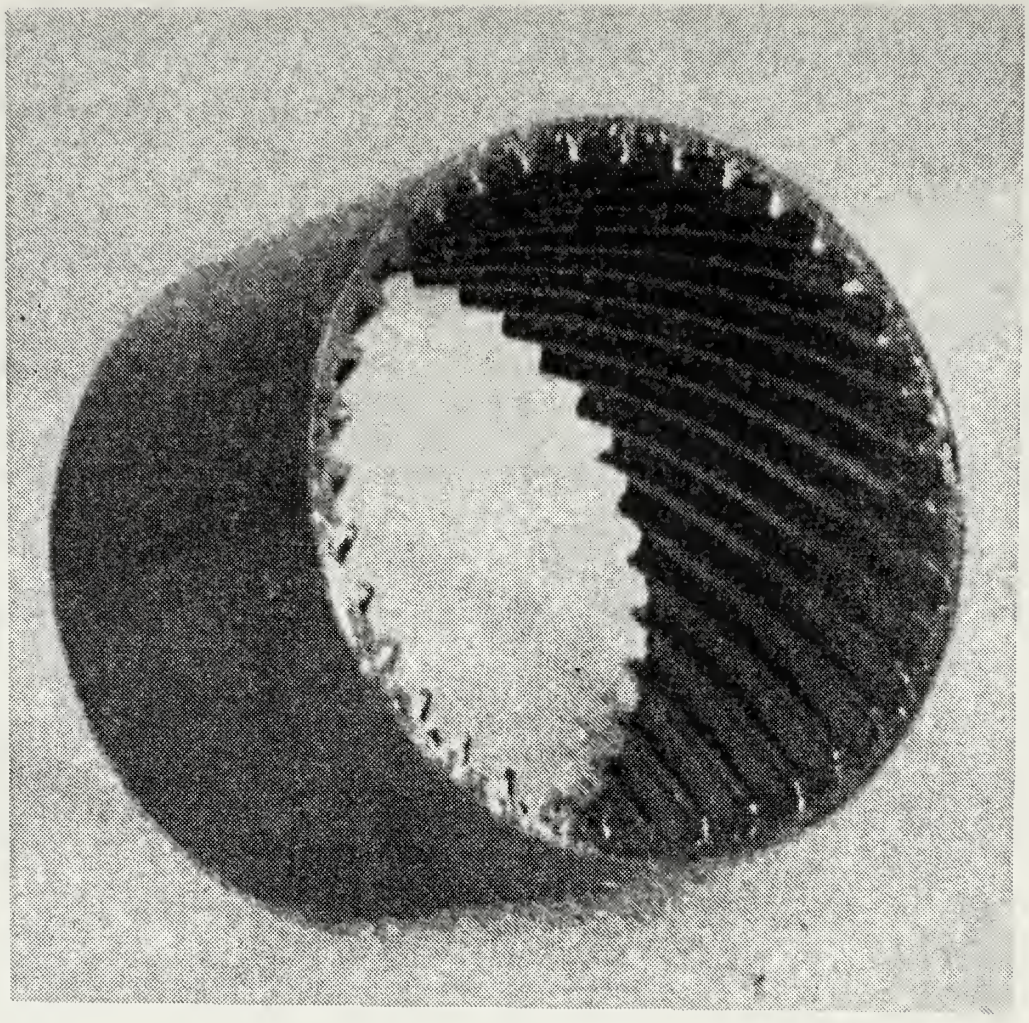

Figure 2-7 Photograph of a Section of the Helical 36 Fin Condenser

TABLE 1.1 SPECIFICATIONS OF THE INTERNALLY FINNED TUBES:

Finning	Number of Fins (mm)	Outside Diameter (mm)	Inside Diameter (mm)	Fin Height (mm)	Fin Thickness (mm)	Helix Angle (degree)	Area Ratios (Comparing to the smooth tube) Outer	Inner (w/o fins)	Inner (with fins)
Straight	22	28.6	25.8	1.35	1.2	0	1.075	1.126	1.437
Helical	16	26.7	24.7	1.80	0.75	26.8	1.003	1.078	1.378
Helical	14	26.5	23.9	2.15	0.75	27.6	0.994	1.043	1.342
Helical	36	25.4	23.8	0.85	0.45	27.0	0.954	1.039	1.200

9. Vacuum and Pressure Test System

Since the experiments were performed under vacuum conditions, any inleakage of noncondensable gases (air) were a serious problem, as also discussed by Gardner [Ref. 10]. Therefore, considerable efforts were made to ensure vacuum-tightness of the system. Vacuum and pressure test lines, shown in Figure 2.8, were used to check for possible leaks. An aluminum test flange was installed in place of the glass view windows. The system was first pressure tested (to about 20psig) with nitrogen. The soap-bubble test was used to locate leaks. After fixing leaks found by the pressure test, a vacuum-hold test was performed over a period of about 10 hours. The system was accepted to be leak-free if the vacuum-lost rate was less than 0.1mm/hr.

For this work, two more test flanges were built to be able to test the evaporator and condenser sections separately. A proper fitting was installed to test the driving-end condenser flange o-ring.

B. INSTRUMENTATION

All temperatures were measured by 30-gage, type-E, teflon- and plastic-coated thermocouple wire. These thermocouples were calibrated using the procedures explained in Appendix B.

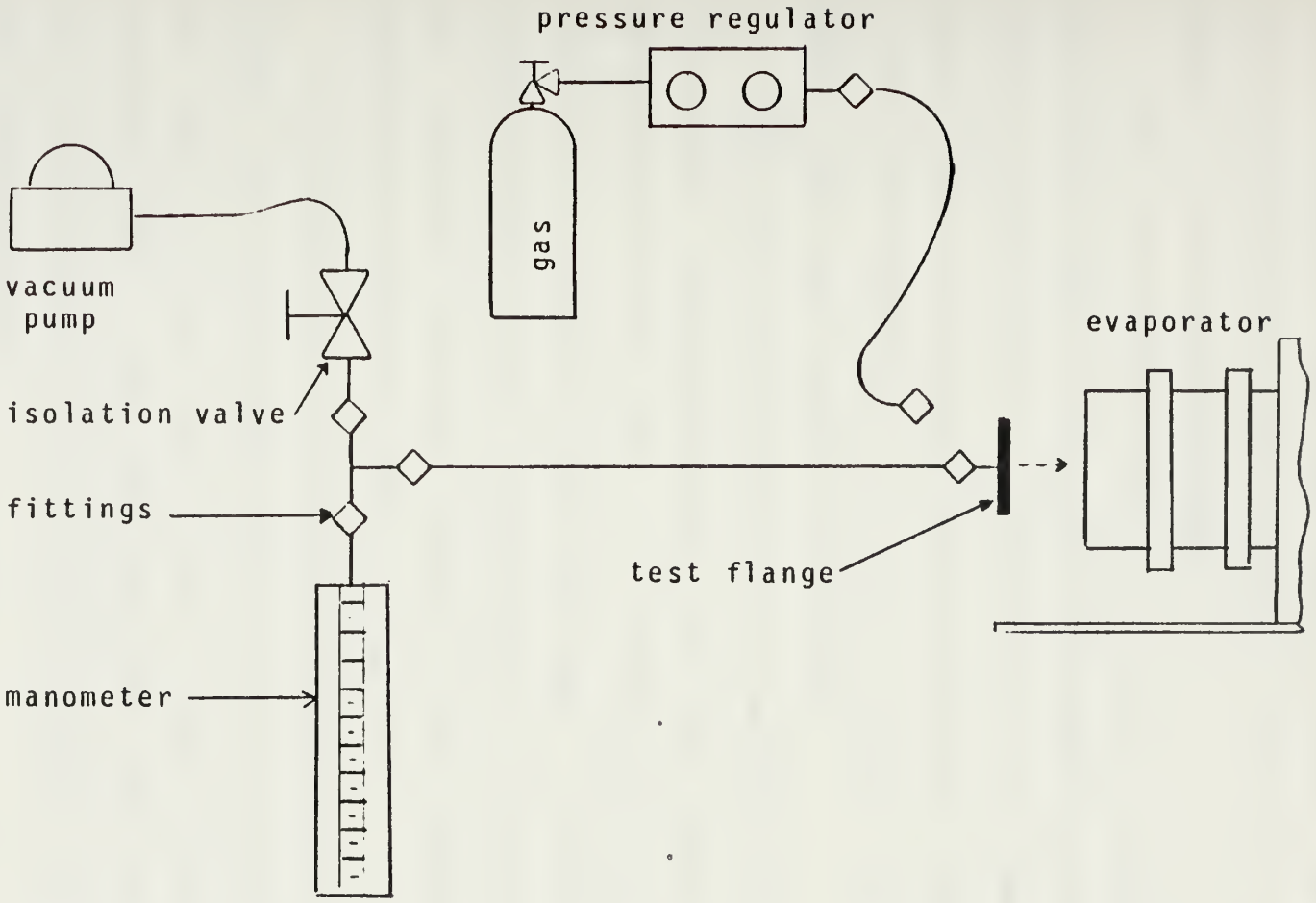

Figure 2.8 Vacuum and Pressure Test System

After making sure that the condenser body and all the silver-soldered connections were air tight, the thermocouples were mounted within axial grooves on the outer surface using the following procedure:

First, the thermocouples were placed in grooves. The grooves were then filled with just sufficient amount of Devcon, type-B epoxy. A greased thin brass sheet was placed over the epoxy and held in place by a strong tape to anchor the thermocouple and epoxy in place. Four hours later these metal sheets were removed.

Vapor space thermocouples were inserted into the two vapor space thermocouple wells until they came in contact with the end of the well. All thermocouple wires were held to the condenser using wire wraps. The wires were passed through holdes in the flange at the drive end of the condenser, and were connected to the cylindrical thermocouple junction boards (Figure 2.9).

To protect wires from breaking apart from the junction board, due to centrifugal force at high rotational speeds, two layers of duct tape were used on the cylindrical junction board. This modification was quite satisfactory with no difficulties as reported by Gardner [Ref. 10] with the previous design.

The wall thermocouple and vapor thermocouple signals were transmitted from the system by a set of viscous, mercury slip rings.

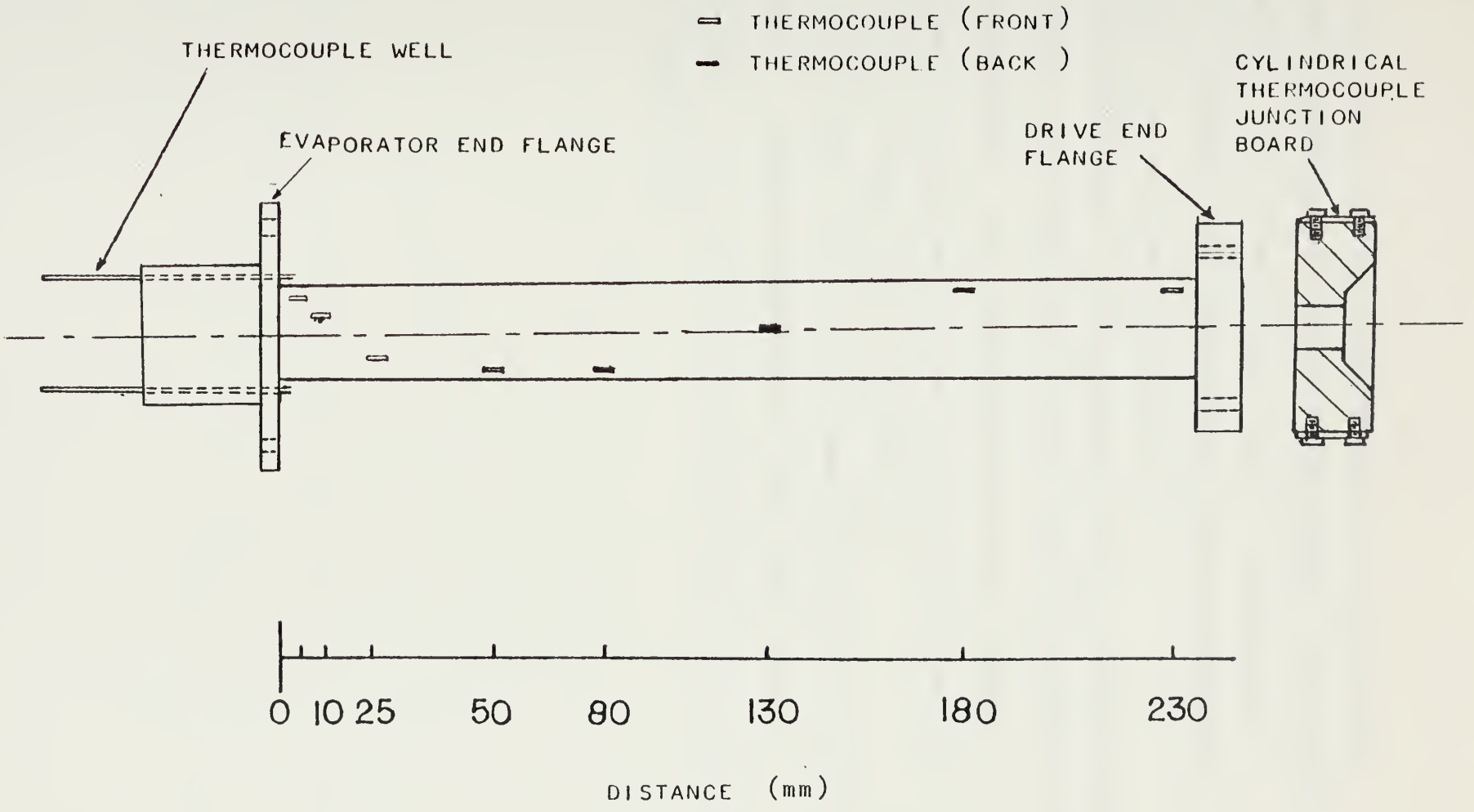

Figure 2.9 Thermocouple Locations

The inlet and outlet temperatures of cooling water were also monitored by type-E thermocouples. The outlet thermocouple consisted of five separate thermocouples wired in parallel, and was inserted into the mixing box discharge line as shown in Figure 2.3.

The thermocouple voltages were read by a Hewlett-Packard (HP) 3054A, data acquisition system, and were entered to an HP-9826 computer. For data acquisition and analysis, a real-time, interactive program was used to reduce and store data on floppy disks [Appendix C].

Cooling water flow rate was measured with a standard rotameter. Accurate regulation of the flow rate was accomplished by adjusting the pressure regulator installed in the cooling line.

III. EXPERIMENTAL PROCEDURES

A. INSTALLATION AND TESTS

1. Inspect all o-rings and o-ring grooves to be sure they are clean and have no flaws.
2. Install the condenser without placing the cooling water box in position.
3. Install the test flange; connect a pressure source and raise the pressure inside the heat pipe to 0.3 MPa (43 psig). Wet the surfaces of all joints thoroughly with soap solution. Inspect all the joints and surfaces for leaks. If there are no leaks evident by the bubble test, follow the pressure gage on the system for 30 minutes. If any leaks are found, take appropriate corrective steps.
4. Disconnect the pressure source and install a vacuum test system. Evacuate the heat pipe, isolate the system and allow it to sit at least 6 hours. Monitor the vacuum in the system to ensure that there are no intolerable leaks.
5. After ensuring that there are no leaks on the condenser, take apart the condenser and install thermocouples.
6. Repeat steps 1-4, but this time place the cooling water box in position.

These tests will detect leaks that may allow non-condensable gases to be inducted into the heat pipe, which operates in a partial vacuum. Daniels and Williams [Ref. 14] have shown that noncondensable gases significantly reduce heat transfer rates in rotating heat pipes.

During the tests of this work, there were no o-ring leaks. But soldered joints produced several leaks which had to be re-soldered to ensure tightness.

B. PREPARATION OF THE HEAT PIPE INTERIOR

1. Remove test flange, tilt the evaporator end down a few degrees to allow the cleaning fluids to run off the heat pipe.
2. Using a brush, scrub the interior of the heat pipe with acetone. Rinse with water thoroughly.
3. Scrub the interior with ethyl alcohol, then rinse with distilled water.
4. Scrub the interior with a solution of equal parts of ethyl alcohol and 50 percent aqueous sodium hydroxide at 80 degrees Celsius. (CAUTION: THIS SOLUTION IS EXTREMELY IRRITANT WHEN CONTACTED BY SKIN. MAKE SURE TO WEAR PROPER EQUIPMENT.) Rinse with distilled water. Check the interior surfaces by spraying water to observe even wetting on the surface.

C. FILLING PROCEDURE

1. Tilt the slip-ring end down about 35 degrees.

2. Pour 300ml of distilled water into the pipe.

3. Dry the glass windows to avoid fogging between them.

4. Place the first glass window on the o-ring. Put the two spacer rings followed by the second window glass and one spacer ring.

5. Tighten the twelve view window retaining bolts consequentially. First, tighten every fifth bolt to 10 inch-lb torque. Then, repeating the procedure. This prevents the cracking of view windows during the installation and experiment.

D. VENTING PROCEDURE

1. Tilt the evaporator end down 30 degrees.

2. Remove the vent screw.

3. Set the power control to 14. Heat the system up to about 100 degrees C.

4. Turn on the data acquisition system and monitor the thermocouple outputs. This gives a chance to check all the thermocouples as the system is heating up. Monitor the vapor temperature (channels 40 and 49) and do not allow this temperature to increase higher than 106 degrees C (6400 μV).

5. When a steady steam flow is observed, out of the vent opening commence timing and allow vemting for 10 minutes.
6. When venting is complete, install the vent screw with o-ring, and turn off power. Turn on the cooling water to cool the system off. Observe violent boiling in the system as it cools down.

E. RUNNING PROCEDURE

1. Bring the system to horizontal position using a level.
2. Wrap the thermocouple junction board with tape to protect the wires from breaking apart due to centrifugal forces.
3. Open the main bearing cooling water valve.
4. Open the needle valve on the oil dripper and adjust the oil flow to 2-3 drops per minute.
5. Open the condenser cooling water and adjust the flow to 40 percent.
6. Energize the computer and the data acquisition system. Load the program (RHPIPE).
7. Energize the frequency counter and set it for rpm display.
8. Pull the drive motor back and adjust for a proper V-belt tension. Rotate system by hand to ensure there is no binding.

9. Start the drive motor and bring the rpm to approximately 1100-1400 to obtain an annulus of water in the evaporator. Then adjust the rpm to the level for this work, data were taken at 700, 1400 and 2800 rpm.

10. Set the power control to a desired level. Monitor one of the vapor space thermocouples; wait ten minutes for system to reach steady-state temperatures. The criterion for steady-state condition is when fluctuation is less than $\pm$ 4 microvolts for any EMF value.

[CAUTION: FOR SAFETY REASONS, DO NOT ALLOW THE VAPOR TEMPERATURE TO EXCEED 106 DEGREE C (6400 μV).].

11. After steady state is reached, take 3 sets of data at each power setting and average these values to reduce the experimental uncertainties.

12. Hand plot heat flux vs. $(T_s - Tc_i)$ to follow data.

F. DATA REDUCTION

Data reduction and analysis are performed by HP 9826 computer using an interactive program written in Basic 2. The original program written by Gardner [Ref. 9] was modified, and a listing of this modified version (Program Name:RHPIPE) is given in Appendix C. This program performs the following steps:

1. Requests the entry of time, rpm, and cooling water rotameter reading. Then samples each thermocouple EMF

twenty times and stores the raw data (mean values) on disk. File for future use.

2. In the analysis portion of the program, corrected temperatures, and in, the cooling water mass flow rate are calculated.

3. The program computes the heat transfer rate (Q) to this cooling water by the following energy balance equation:

$$Q = \dot{m} * C_p * (T_{co} - T_{ci}) - Q_f$$

where

Q = Heat transfer rate from condensing vapor [W]

$\dot{m}$ = Cooling water mass flow rate, [kg/s]

C_p = The specific heat of water, [kJ/kg-K]

T_{co} = The cooling water outlet temperature, [Degree C]

T_{ci} = The cooling water inlet temperature, [Degree C]

Q_f = Frictional heat rate generated in the system by friction, when zero power applied. [W]

4. The program displays the following output neither short or long format. Short format is used to make a table or results. Long format displays all individual thermocouples which enables the user to check if all the thermocouples work properly:

Q	watts
$T_s - T_{c_i}$	degrees C
$T_s - T_{wall}$	degrees C
$T_{wall} - T_{avg}$	degrees C
$T_{co} - T_{ci}$	degrees C

6. The program stores the results on a disk file for future use.

IV. PRESENTATION AND DISCUSSION OF RESULTS

A. GENERAL COMMENTS

Five different condensers were tested for this thesis. To determine the heat transfer rate due to friction at the bearings, each condenser was tested at 700, 1400 and 2800 rpm with no power to the evaporator. The frictional heat transfer rate (Q_f) for each condition was calculated from the heat balance applied to cooling water.

Heat transfer rate (Q) versus the difference between saturation temperature and cooling water inlet temperature ($T_s - T_{ci}$), which is the driving potential temperature difference, were plotted. Data were taken incrementally for increasing and decreasing power settings.

Computer outputs for all runs are tabulated in Appendix C.

B. RESULTS OR SMOOTH WALL CONDENSER

Figure 4.1 and Tables C1, C2, and C3 show the results of the smooth wall condenser. This condenser was chosen to provide a base performance to compare to the internally finned condensers. As expected, data correlate well with the work of Wiegel [Ref. 9] and Wagenseil [Ref. 7].

The heat transfer rate shows the improvement with rpm. For a rotating cylinder, the condensate flow is induced by the pressure gradient established in the condensate as a

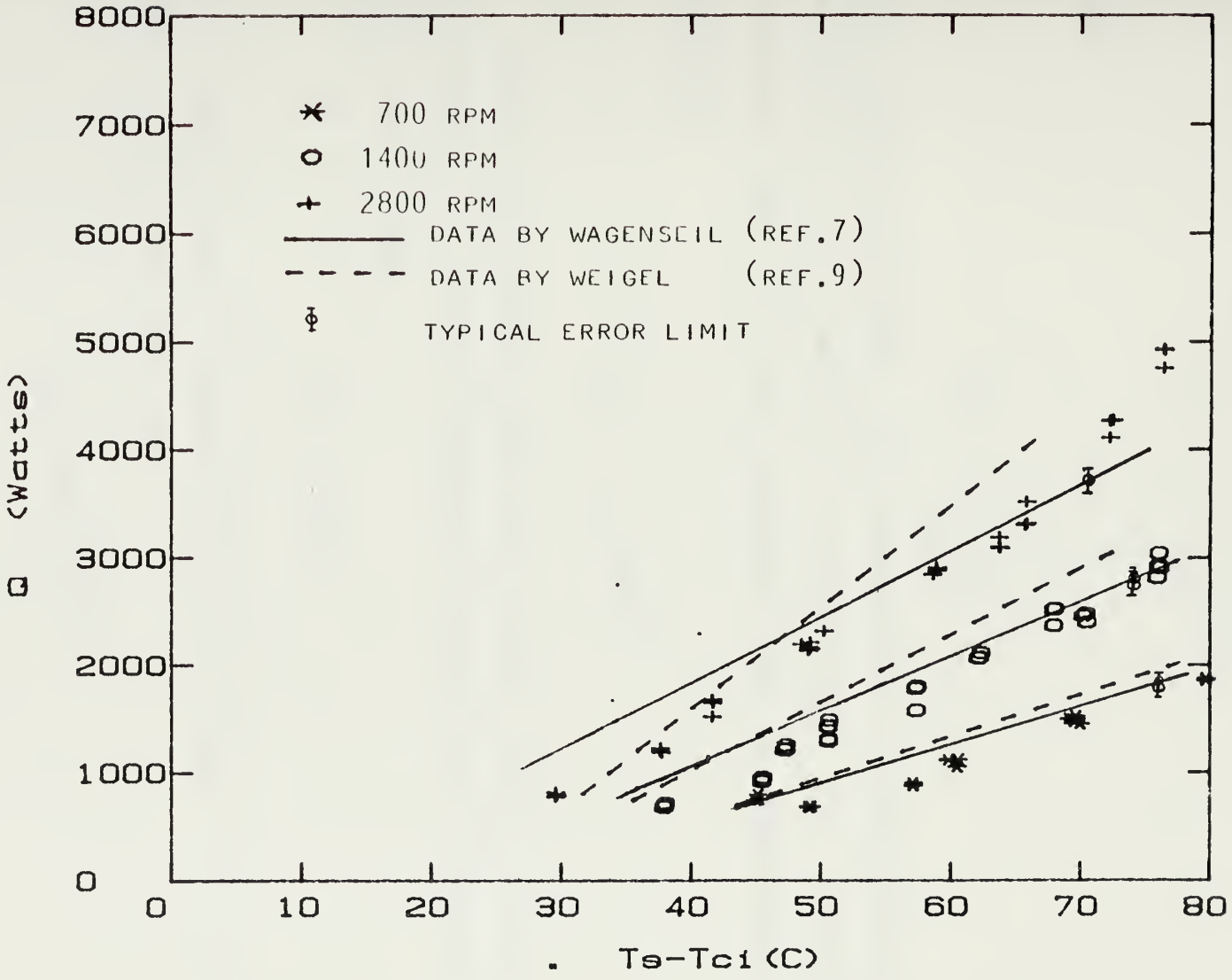

Figure 4.1 Smooth Condenser Thermal Performance

result of its variable film thickness. Leppert and Nimmo [Refs. 11 & 12] have shown, that for condensation on a flat plate at a constant surface temperature:

$$Nu_T = 0.64\ Sh_T^{1/5}$$

where

$$Sh_T = \frac{g\rho^2 h_{fg}\ L^3}{k\Delta T\mu}$$

For a rotating cylinder, the gravitational acceleration may be replaced by the centrifugal acceleration, $\omega^2 r$. Roetzel and Newman [Ref. 13] (for a rotating drum) recommended the relation:

$$Nu_T = 0.78\ Sh^{1/5}$$

These relationships show that the heat transfer rate on the inside of a rotating cylinder increases with increasing RPM, specifically;

$$Nu_T \propto RPM^{2/5}$$

In a similar way, for constant heat flux, Nimmo and Leppert [Refs. 11 and 12] also give;

$$Nu_q = 0.75\ Sh^{1/4}$$

and Roetzel and Newman [Ref. 13] give:

$$Nu_q = 0.62\ Sh^{1/4}$$

where

$$Sh_q = \frac{g\rho^2 h_{fg} L^2}{\mu \dot{q}}$$

$$\dot{q} = \text{heat flux } (Q/A_i)$$

Therefore, in this situation

$$Nu_q \alpha RPM^{1/2}$$

In addition, the water-jet cooling on the outside of the condenser surface may, as an approximation, be treated in a similar way to steam condensation on a rotating cylinder. This problem was investigated by Nicol and Gacesa [Ref. 14]. They show that for high rotational speeds (i.e., Weber numbers greater than 500),

$$\frac{h_o D_o}{k} = 12.26\ We^{0.496}$$

where

$$We = \rho\omega^2 D_o^3/4\sigma g$$

The outside heat-transfer coefficient is, therefore, proportional to the Weber number raised to 0.496 power so it is almost proportional directly to RPM.

Hence, with increasing rotational speeds both internal and external heat-transfer coefficients must increase.

To compare the theoretical and empirical results, Log-Log plots of the Nusselt versus Sherwood number were made as shown in Figures 4.2 and 4.3.

For this comparison, the following simplifications were made:

1. The condenser outside wall temperature was taken as the unweighted average of all thermocouple readings.
2. All fluid properties were evaluated at the film temperature.

$$T_f = \frac{T_s + \overline{T}_{wi}}{2}$$

where $\overline{T}_{wi}$ is the average inside wall temperature (K).

3. Heat flux through the condenser was considered uniform.

The average inside heat transfer coefficient was therefore

$$h_i = \frac{Q}{A_i [T_s - \overline{T}_{wi}]}$$

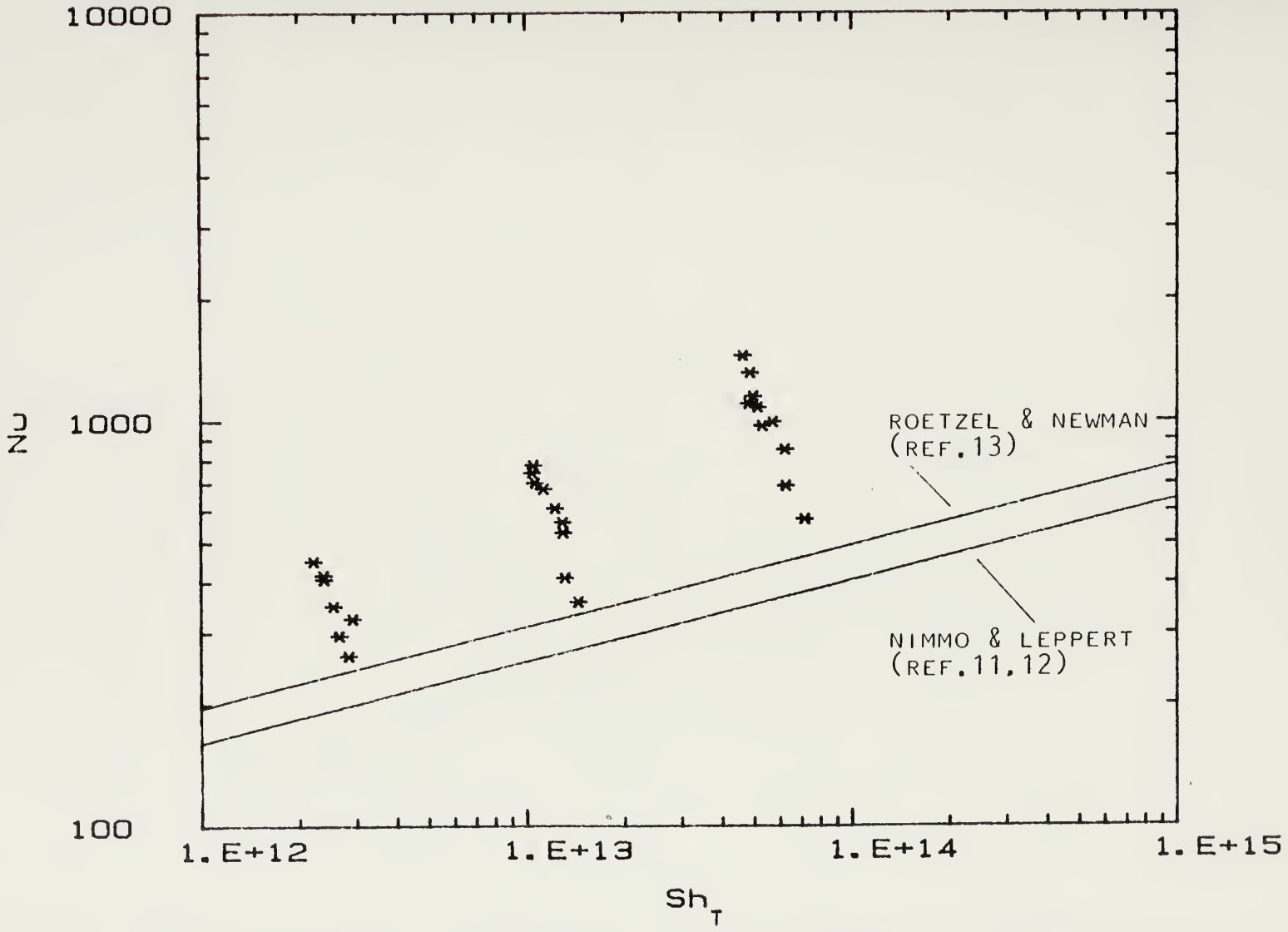

Figure 4.2 Sherwood Number vs. Nusselt Number for Constant Wall Temperature.

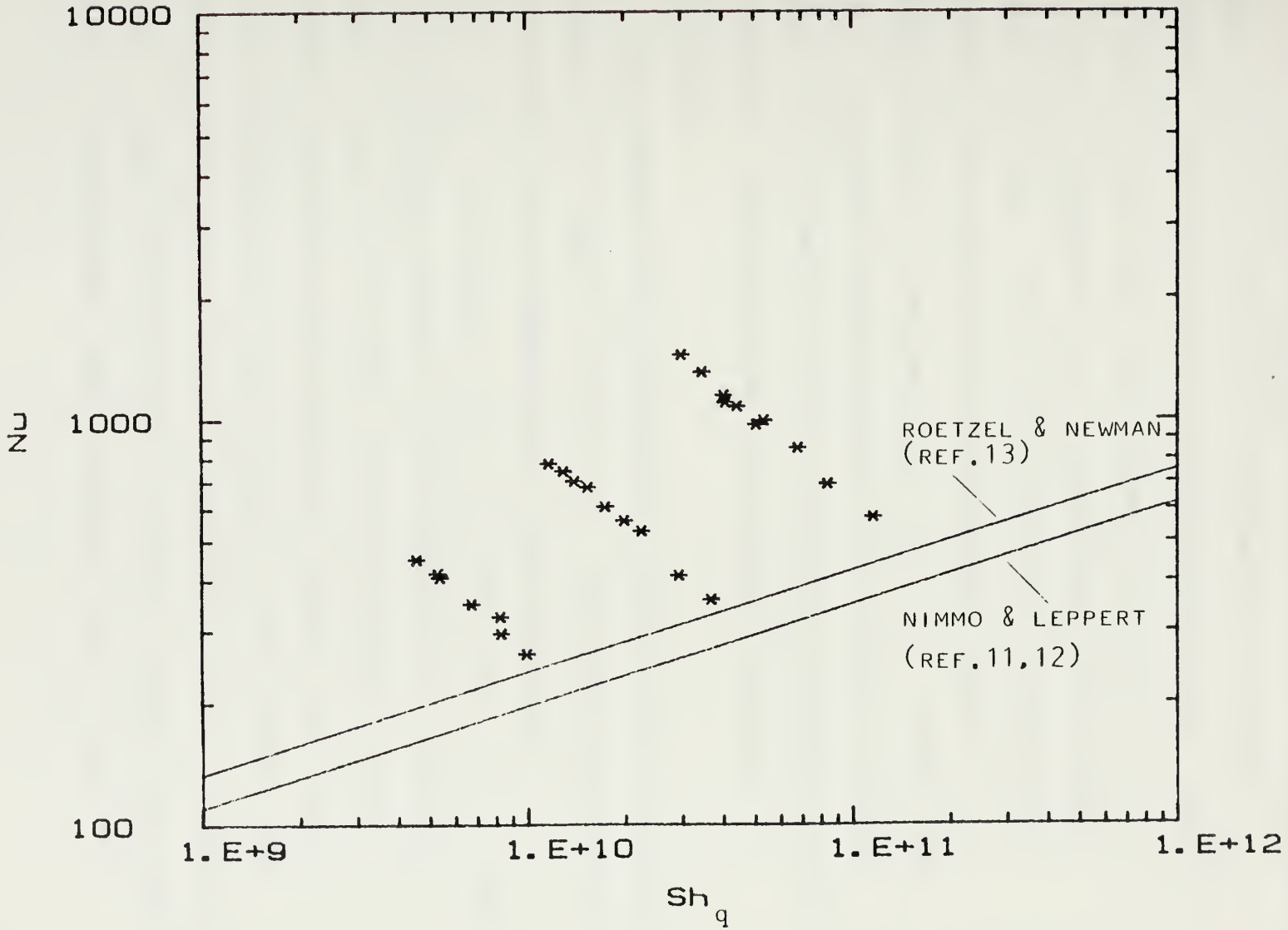

Figure 4.3 Sherwood Number vs. Nusselt Number for Constant Wall Heat Flux.

The mean Nusselt number, $Nu = \bar{h}_i L/k$ for a given heat transfer rate was determined from the data and the Sherwood number was calculated with the assumption of either constant wall temperature or constant heat flux. Figures 4.2 and 4.3 show that, for a given set of data, as $(T_s - \bar{T}_{wi})$ increases (i.e., Sh decreases), the Nusselt number increases. This trend disagrees with empirical equations, but agrees well with the data trend of Wagenseil [Ref. 7] and Tantrakul [Ref. 8]. On the other hand, the overall trend from one set of data to another shows that the Nusselt number increases as Sherwood number increases. The reason for this unusual discrepancy is not known.

The condenser wall temperature profiles for the smooth condenser are shown in Figure 4.4. This plot was made for the values of wall temperature at the condition of $(T_s - T_{ci}) = 70$ degrees C for all three RPM's. At all RPM's, the temperature closest to the evaporator is a maximum. This is caused by the heat conducted through the main bearings (heat from the evaporator and the frictional heat generated in the main bearing) if one neglects the temperature at 5mm. From the evaporator end, the remaining profiles are relatively flat to 130mm. And then they drop off to a temperature close to that of the cooling water.

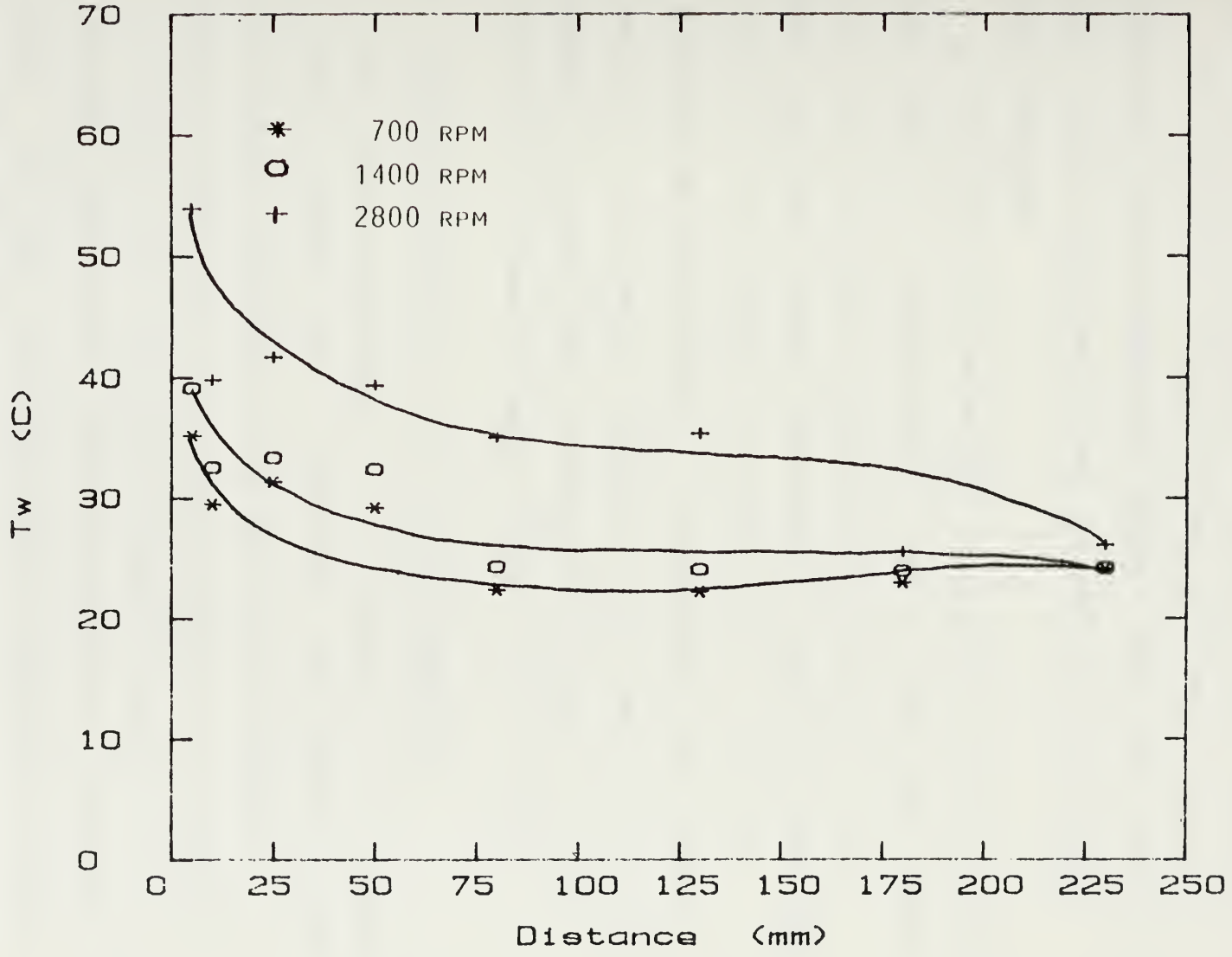

Figure 4.4 Wall Temperature Distribution of Smooth-Wall Condenser at 90 Degree C Saturation Temperature.

C. RESULTS OF THE STRAIGHT 22-FIN CONDENSERS

The heat transfer rates, determined for the 22-fin condenser at 700, 1400 and 2800 RPM are shown in Figure 4.5.

This condenser showed the best performance among the internally-finned condensers tested. These data show up to a 230 percent improvement over the data for the smooth-wall condenser.

In examining the geometrical properties of this finned tube (Table 2.1), notice that it has an area ratio (total inside area to smooth condenser inside area) of 1.437. Hence, the heat transfer improvement results are more than just due to the increase of surface area. Since the conditions on the outside of this condenser were almost identical to the smooth condenser case, then the observed increase in overall heat transfer must be due to a more significant increase in heat transfer on the inside.

D. RESULTS OF HELICAL 14 and 16 FIN CONDENSERS

The thermal performance of the helical 16-fin condenser is shown in Figure 4.6. At 2800 RPM, this condenser shows a 110 percent improvement over the smooth condenser. By helically finning the tube wall in addition to increasing the internal area, the counter-clockwise spiral acts as a condensate pump when the shaft is rotated in a clockwise fashion. The fins, therefore, act as impellers to force the condensate back to evaporator instead of relying upon

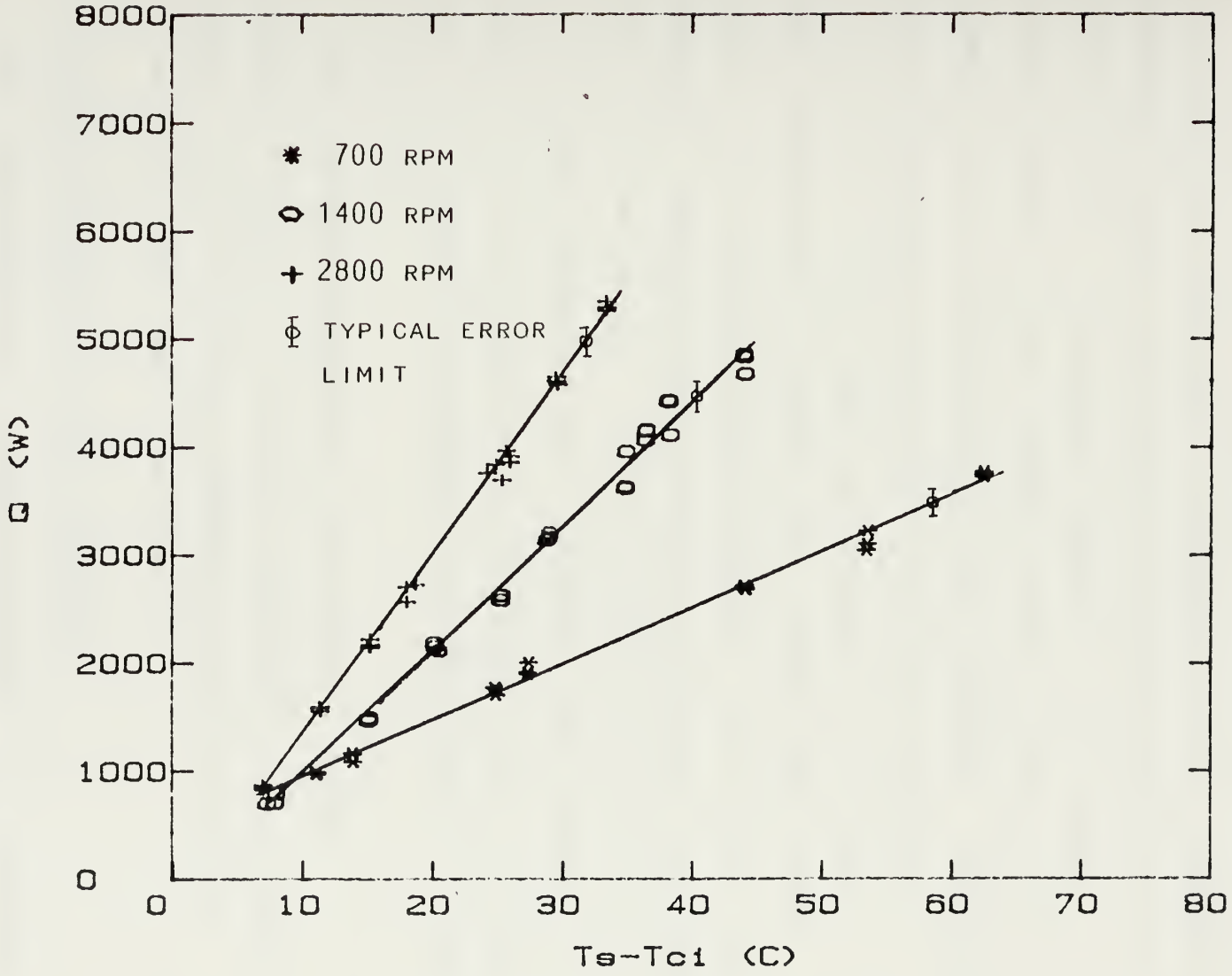

Figure 4.5 Straight 22-Fin Condenser Thermal Performance

hyrostatic pressure. But this effect did not improve the performance as much as the straight fin condenser except for the 700 RPM case. Obviously, this pumping effect was not dominant at higher RPM. The reason for this unexpected phenomenon became clear when the interior surface of the spirally-finned condenser was examined. The surface between the fins is much rougher on the spirally-finned condenser then on the straight-finned condenser. Apparently, during fabrication of the helically-finned condenser, a series of transverse ridges are created in the trough region between fins, (Figure 2.5). These ridges do not appear in the straight finned condenser. As a result, the condensate undergoes more frictional resistance when flowing back to the evaporator. This extra resistance thicknes the film and reduces the heat transfer. Also, since the helical fins were thinner than the straight fins, they may not be as effective in condensing the vapor due to a lower fin efficiency.

The thermal performance of the helical 14-fin condenser (Figure 4.7) is almost identical to the results (Figure 4.6) of the 16-fin condenser with very similar fin geometry, helix angle and diameter.

E. RESULTS OF HELICAL 36-FIN CONDENSER

For this condenser, as shown in Figure 4.8, a thermal improvement of up to 40 percent over the smooth condenser

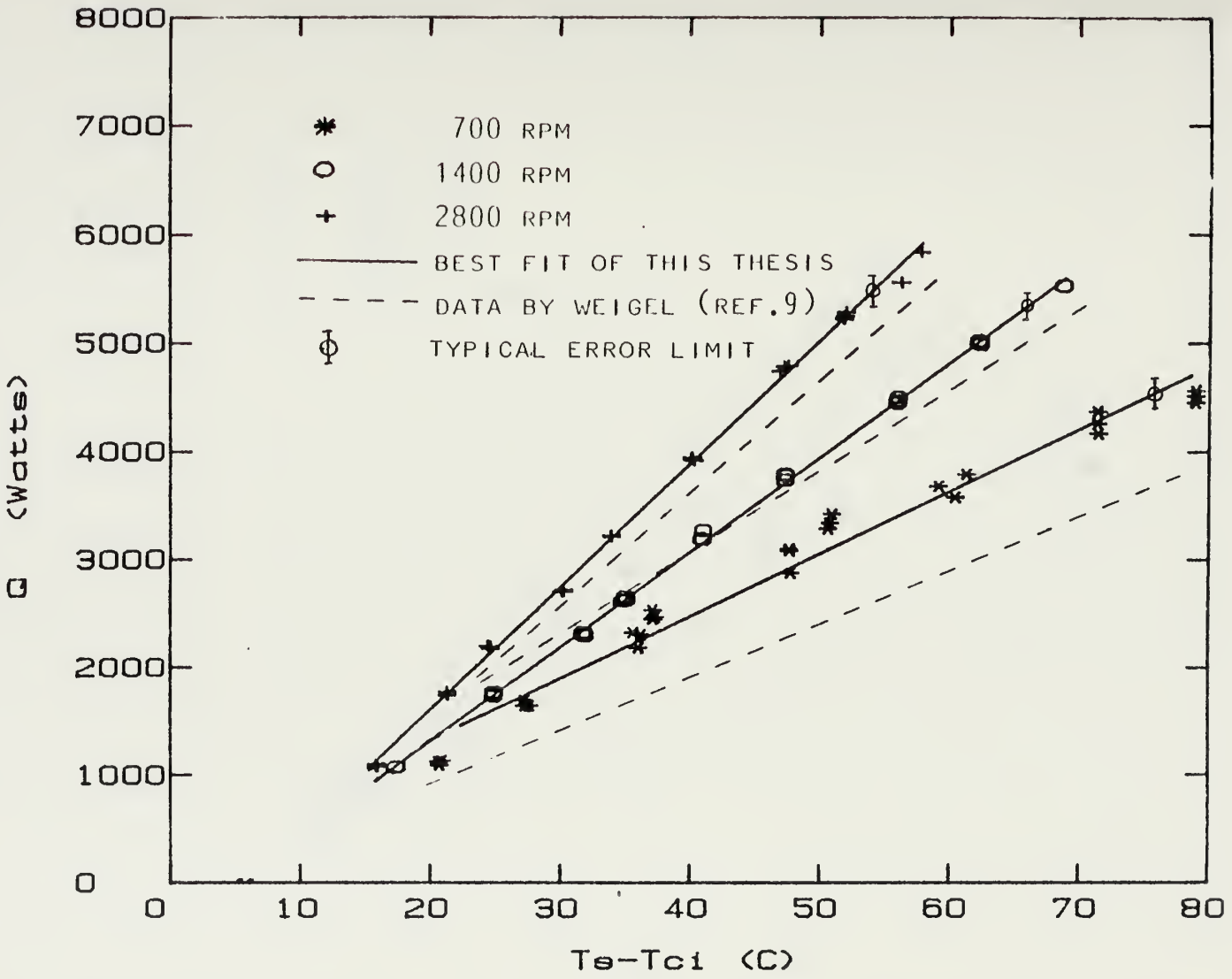

Figure 4.6 Helical 16-Fin Condenser Thermal Performance

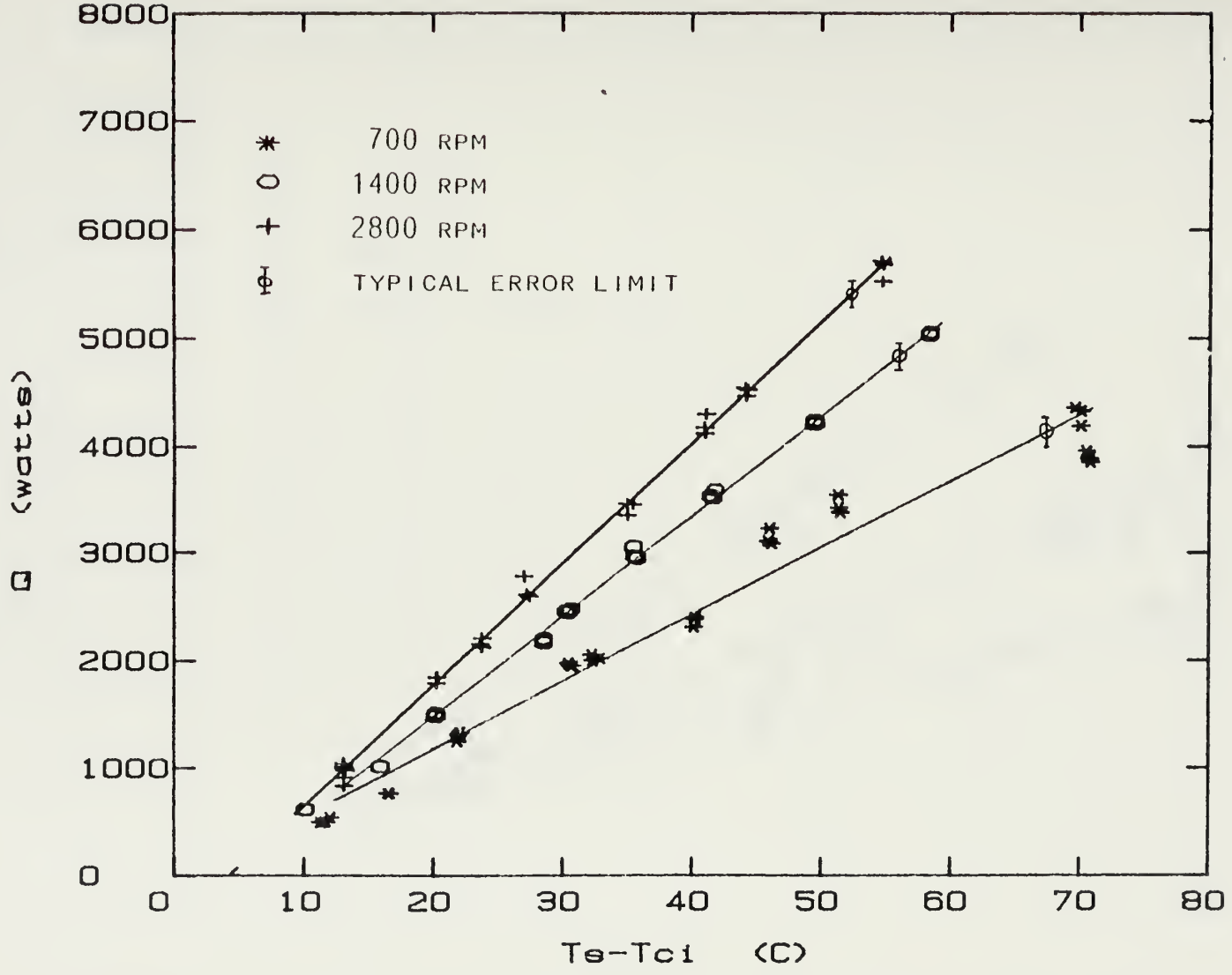

Figure 4.7 Helical 14-Fin Condenser Thermal Performance.

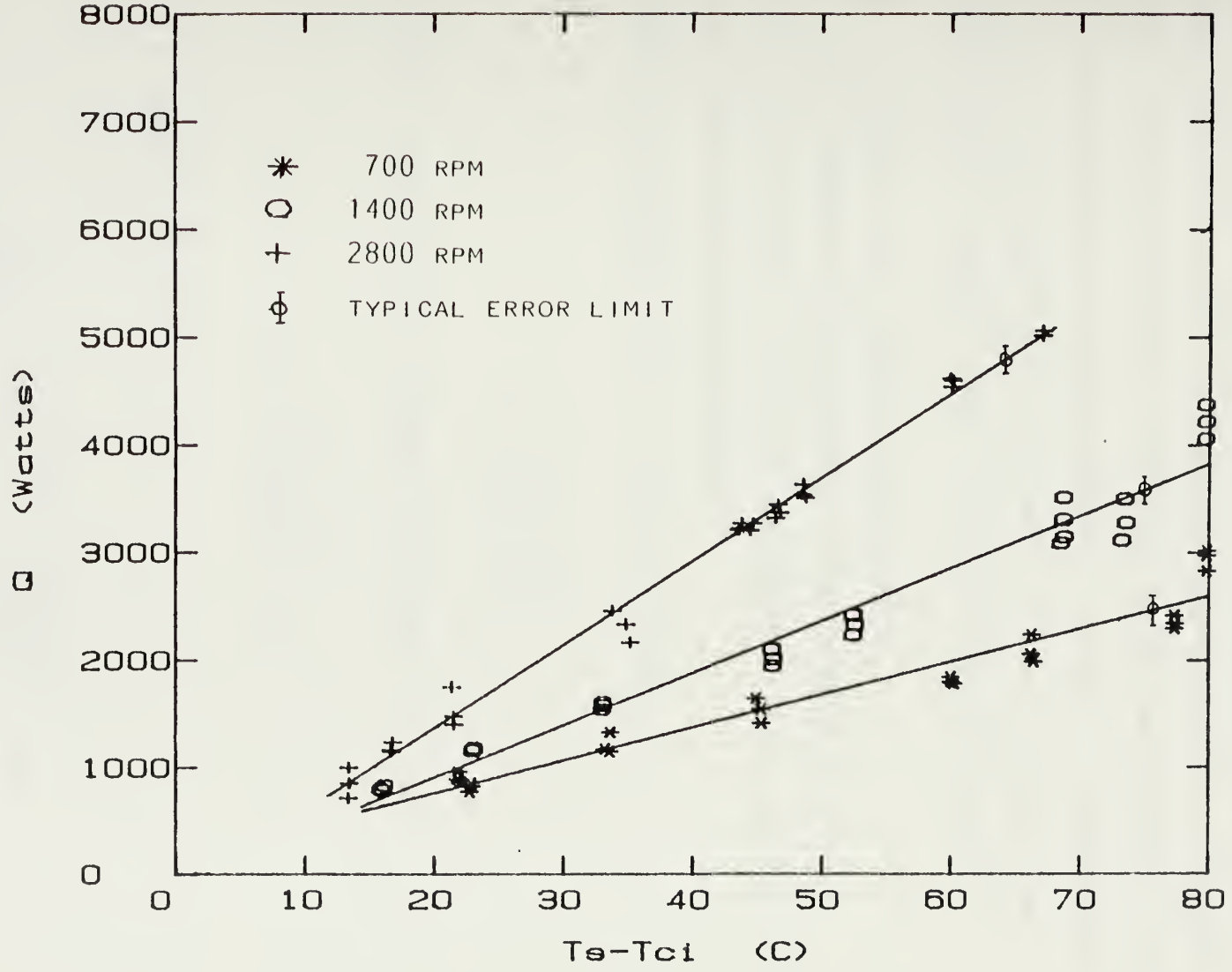

Figure 4.8 Helical 36-Fin Condenser Thermal Performance.

is evident. This can be explained since the fin height of this condenser is the smallest with 0.85mm. For this case, the condensate thickness at the trough may cover a large portion of the fin height, decreasing its effectiveness for heat transfer since most of the condensation occurs at the portion of the fin exposed to vapor. Due to this reason, the improvement obtained on this condenser was considerably smaller than for pipes with high fins.

F. INTERNAL HEAT TRANSFER ENHANCEMENT

The internal heat-transfer coeeficients of the internally-finned and smooth condensers were calculated, by using the following procedure:

The heat transfer rate Q may be written:

$$Q = \frac{T_s - \overline{T}_{wo}}{R_i + R_w}$$

so that the internal thermal resistance R_i is:

$$R_i = \frac{T_s - T_{wo}}{Q} - R_w \quad .$$

As a result, we may write:

$$\frac{1}{h_i A_1} = \frac{T_s - \overline{T}_{wo}}{Q} - \frac{\ell n(r_o/r_i)}{2\pi L k_w}, \quad \text{or}$$

$$h_i = \left[A_i \left(\frac{T_s - \bar{T}_{wo}}{Q} - \frac{\ell n(r_o/r_i)}{2\pi L k_w} \right) \right]^{-1}$$

where

A_i = Inside surface area, m^2 .

r_o = Outside radius , m .

r_i = Inside radius, m .

k_w = Thermal conductivity of wall, W/m.K .
(Assumed at 300 K for calculations.)

L = Effective length of condenser, m .

The internal heat transfer coefficient ratio of the internally finned to smooth wall condenser, (h_f/H_s) are ploted versus driving temperature difference $(T_s - T_{ci})$ in Figures 4.9 - 4.12. Figure 4.9 shows the variation for the straight 22 fin condenser while Figures 4.10, 4.11, and 4.12 show the plots of the helically finned condensers. Based upon the plots obtained, the following observations are made:

1. At low temperature differences, larger enhancements were observed due to very thin films on fins and in the troughs. As the temperature difference increases the films become thicker and this, of course, reduces the internal enhancement.

2. The highest enhancement was observed for the straight 22-fin condenser with the highest area ratio (Figure 4.9). Also, for the helical 36-fin condenser with the lowest area ratio enhancement reaches the smallest level.

3. In all the finned condensers, at low temperature differences (where the enhancement is larger) the heat transfer coefficient ratio improves when the rotational speed is increased from 700 to 1400 rpm. But the ratio is somewhat less significant at 2800 rpm.

The reason for this is the expection of more flow in the trough with increasing rpm.

At low rotational speeds, with lower flow rate, the film thickness in the trough section will be smaller. But at very high rotational speeds, the thinner films on the fin tips cause thicker films in the trough section.

But this phenomenon has to be further studied with future experiments. Using a finite element code to examine the rpm effect on the internal heat-transfer coefficient ratio will be an enlightening study.

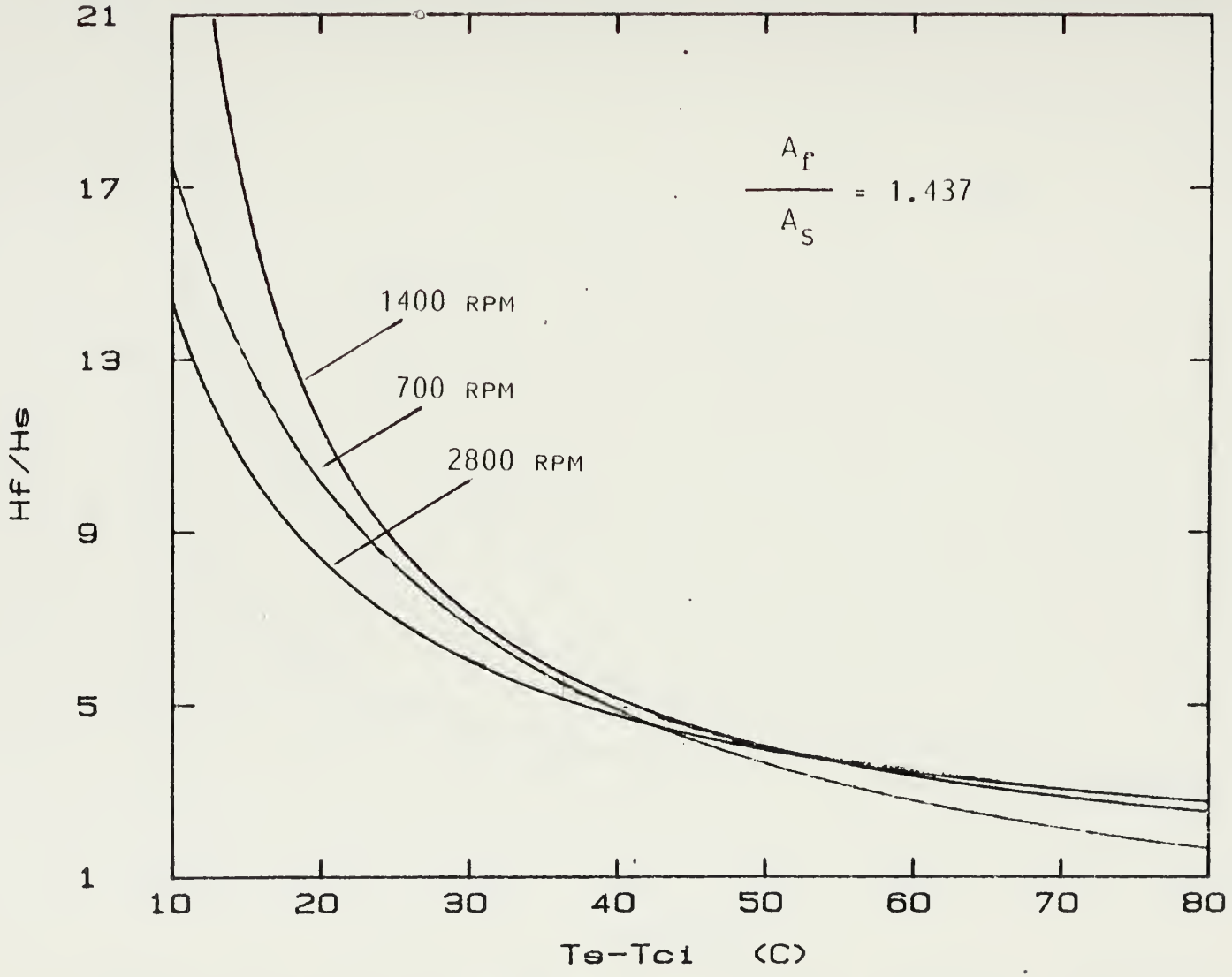

Figure 4.9 Internal Enhancement of Straight Fin Condenser

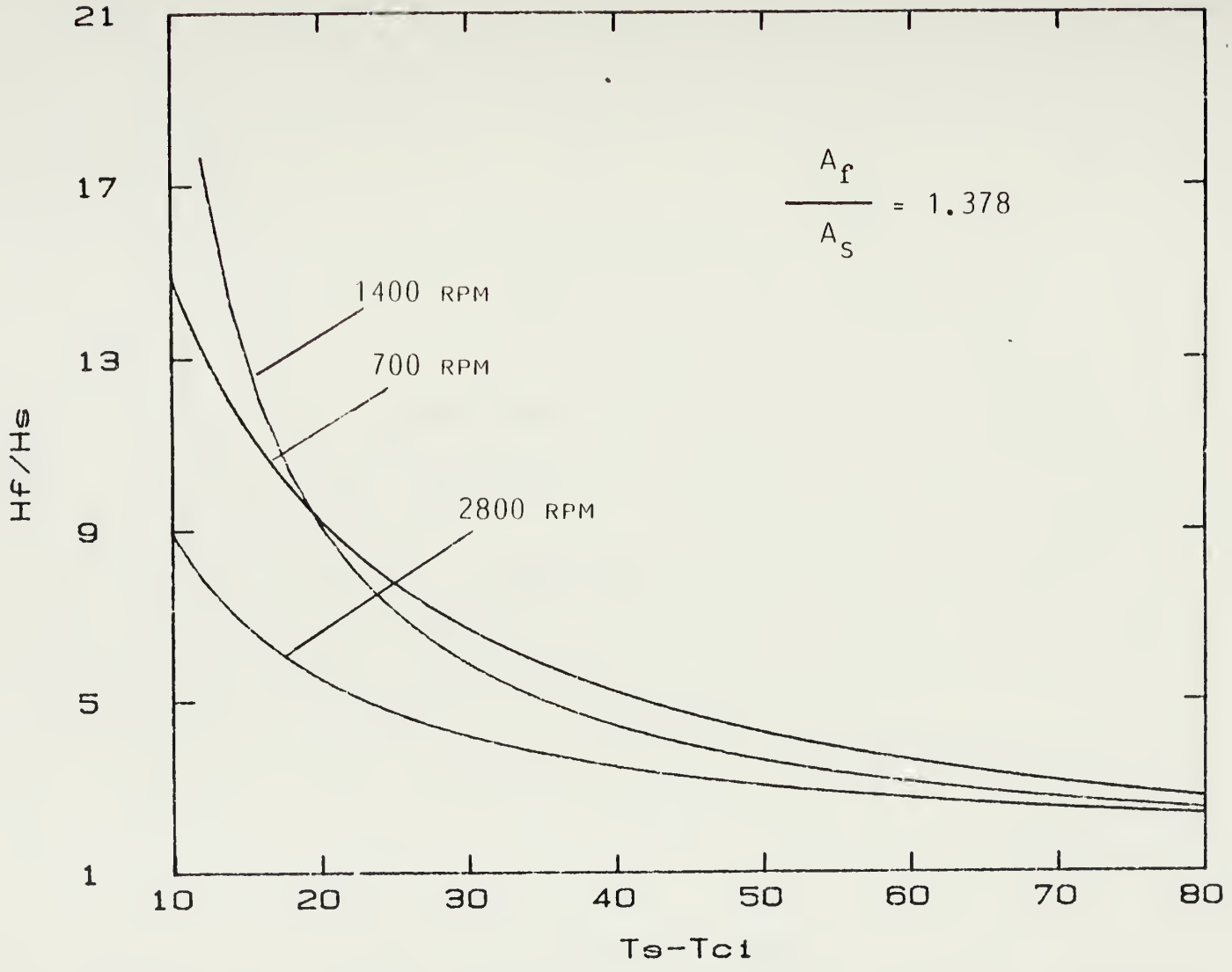

Figure 4.10 Internal Enhancement of Helical 16 Fin Condenser

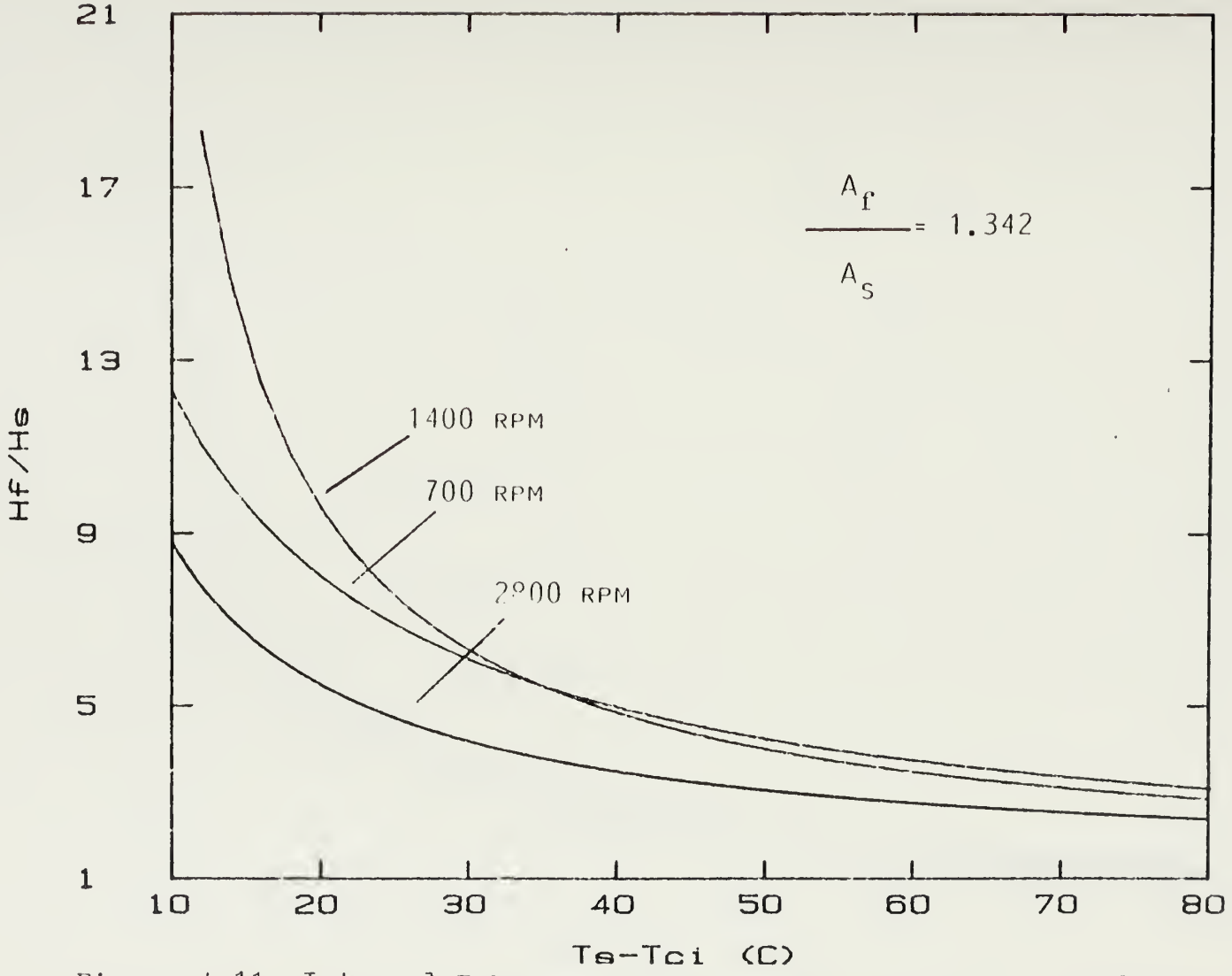

Figure 4.11 Internal Enhancement of Helical 14 Fin Condenser

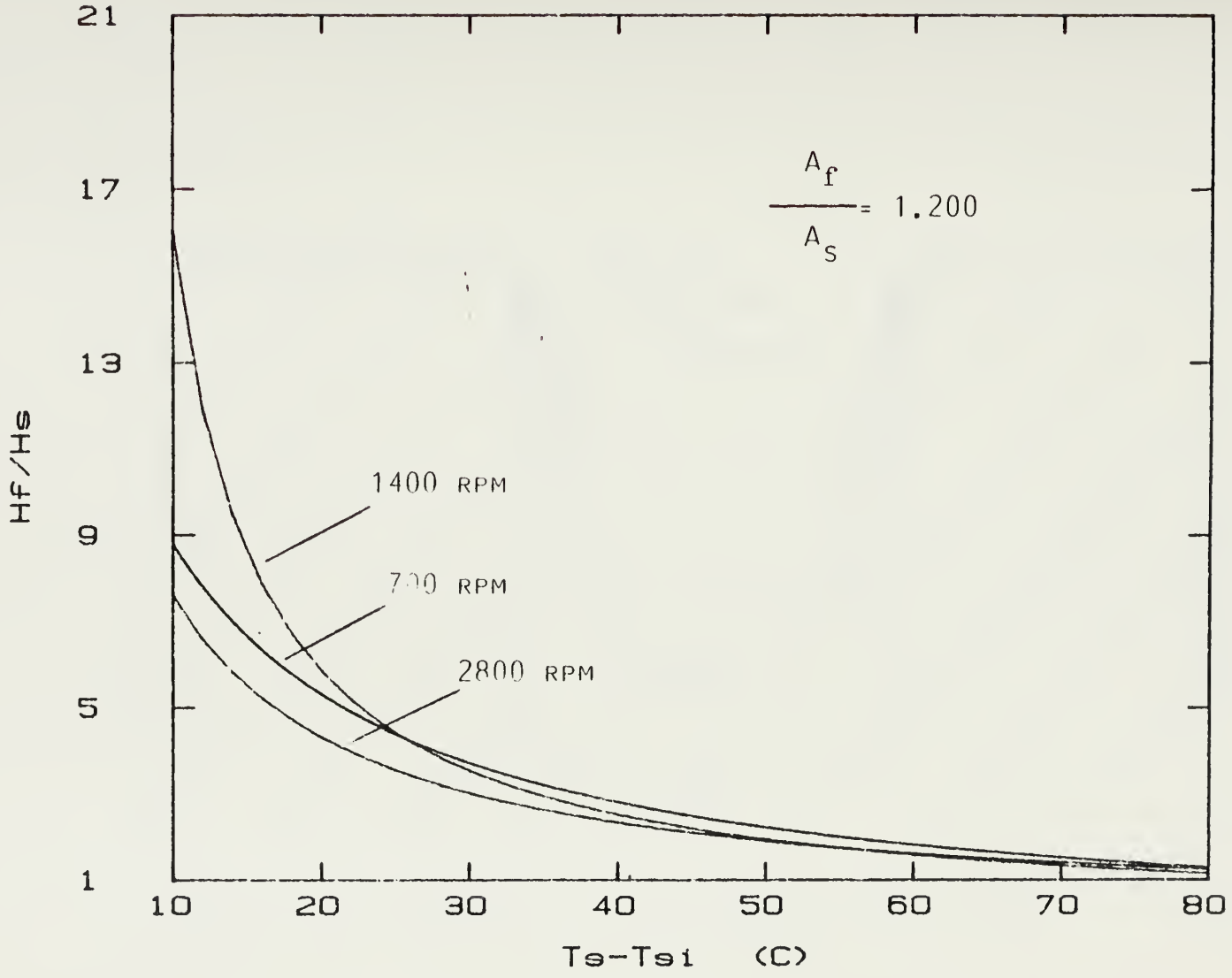

Figure 4.12 Internal Enhancement Of Helical 36 Fin Condenser

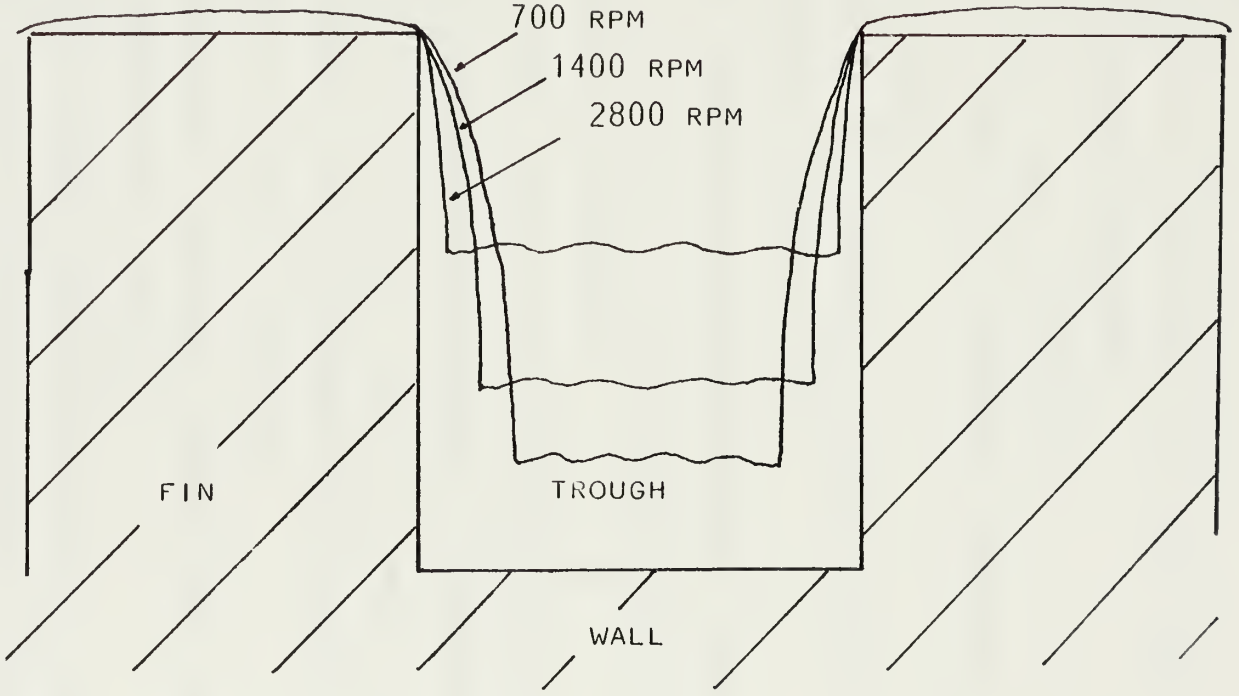

Figure 4.13 Variation of Film Thickness with RPM

V. CONCLUSIONS AND RECOMMENDATIONS

A. CONCLUSIONS

The following conclusions have been made based on the experimental results obtained:

1. At 2800 rpm, $T_s - T_{ci} = 30$ degree C,

   a. Helical 14 and 16 fin condenser performance improved by 110 percent.

   b. Straight 22 fin condenser provided the best performance improvement with 230 percent.

2. At 700 rpm, the heat-transfer-performance improvement for helical 14 and 16 fin and the straight fin performance increased as much as 225 percent.

3. Length of trough section and fin height play and important role on condenser performance. Condensers with small fin height, fin thickness, and with small trough section don't improve the performance significantly even though the number of fins is increased.

4. As rotational speed increases, internal and external heat transfer coefficients increase.

5. Internal heat-transfer-coefficient ratio of internally-finned condenser versus smooth wall condenser varies from 2 up to 20 depending on $(T_s - T_{ci})$ and rpm.

TABLE C.5

Results of Straight 22 Fin Condenser at 1400 rpm

Month, date and time: 11:21:10:00:51
Rotor speed = 1400
Rotameter reading = 35.0

Data Set #	Tci (C)	Tco (C)	Dcw (C)	Ts (C)	Tw (C)	Dmax (C)	Q (W)
1	21.23	22.69	1.46	31.28	26.76	10.05	743.09
2	21.23	22.55	1.32	30.34	26.29	9.11	652.27
3	21.24	22.57	1.33	31.14	26.65	9.90	658.61
4	21.24	23.78	2.54	40.18	30.70	18.95	1442.46
5	21.23	23.73	2.50	40.15	30.80	18.92	1414.20
6	21.23	23.73	2.50	40.16	30.74	18.93	1417.43
7	21.23	25.53	4.30	52.79	36.67	31.57	2585.12
8	21.22	25.46	4.23	52.88	36.67	31.66	2539.92
9	21.23	25.53	4.30	52.91	36.64	31.68	2585.10
10	21.21	27.56	6.36	64.87	42.13	43.66	3915.68
11	21.21	27.07	5.85	64.78	42.20	43.57	3588.84
12	21.21	27.04	5.83	64.84	42.16	43.63	3575.67
13	21.20	28.93	7.73	76.19	47.40	54.99	4806.66
14	21.20	28.90	7.70	76.27	47.25	55.07	4783.38
15	21.20	28.65	7.45	76.34	47.31	55.14	4623.57
16	21.18	26.97	5.79	69.10	43.18	47.92	4064.17
17	21.17	27.38	6.21	69.00	43.18	47.82	4372.52
18	21.19	27.41	6.22	68.89	43.20	47.70	4381.32
19	21.17	27.01	5.85	66.77	42.08	45.60	4102.39
20	21.15	27.01	5.86	66.77	42.05	45.62	4112.27
21	21.16	26.89	5.73	66.72	42.07	45.56	4017.43
22	21.14	25.70	4.57	57.38	37.86	36.25	3161.11
23	21.14	25.65	4.51	57.36	37.92	36.22	3119.40
24	21.15	25.64	4.48	57.14	37.83	35.99	3100.46
25	21.15	24.24	3.09	46.76	33.05	25.62	2074.46
26	21.15	24.29	3.14	46.45	33.02	25.30	2110.22
27	21.15	24.34	3.19	46.34	33.10	25.20	2146.58

NOTE: Above analysis was performed for data in file S22FP_2

TABLE C.6

Results of Straight 22 Fin Condenser at 2800 rpm

Month. date and time: 11:21:10:03:09
Rotor speed = 2800
Rotameter reading = 40.0

Data Set #	Tci (C)	Tco (C)	Dcw (C)	Ts (C)	Tw (C)	Dmax (C)	Q (W)
1	21.16	22.57	1.41	29.89	26.54	8.73	835.12
2	21.16	22.57	1.42	29.98	26.62	8.82	762.63
3	21.15	22.61	1.45	29.99	26.60	8.84	788.78
4	21.14	23.54	2.40	35.40	29.48	14.26	1482.87
5	21.15	23.60	2.45	35.42	29.48	14.28	1524.71
6	21.14	23.58	2.44	35.33	29.43	14.18	1515.63
7	21.09	24.87	3.78	43.63	33.85	22.54	2502.83
8	21.09	25.09	4.00	44.48	33.96	23.39	2666.91
9	21.11	25.08	3.97	43.66	33.93	22.56	2643.71
10	21.09	26.40	5.31	52.30	38.69	31.71	3632.39
11	21.09	26.49	5.40	51.42	38.51	30.33	3698.22
12	21.09	26.60	5.51	52.19	38.70	31.09	3777.92
13	21.11	28.58	7.47	62.38	44.37	41.76	5220.80
14	21.11	28.66	7.55	62.91	44.22	41.79	5278.50
15	21.13	28.56	7.43	62.89	44.27	41.76	5191.06
16	21.13	27.67	6.54	58.05	41.65	36.92	4538.75
17	21.10	27.70	6.59	58.07	41.71	36.97	4576.45
18	21.12	27.62	6.50	58.18	41.62	37.06	4509.38
19	21.10	26.78	5.69	53.21	38.83	32.12	3906.45
20	21.09	26.62	5.53	53.57	39.15	32.48	3795.44
21	21.07	26.68	5.61	53.59	39.22	32.51	3849.99
22	21.11	24.35	3.24	40.17	31.93	19.06	2104.07
23	21.11	24.42	3.31	40.14	31.90	19.04	2159.86
24	21.11	24.31	3.20	40.17	31.90	19.06	2078.68

NOTE: Above analysis was performed for data in file S22FP_3

TABLE C.7

Results of Helical 16 Fin Condenser at 700 rpm

Month, date and time: 11:21:10:54:06
Rotor speed = 700
Rotameter reading = 40.0

Data Set #	Tci (C)	Tco (C)	Dcw (C)	Ts (C)	Tw (C)	Dmax (C)	Q (W)
1	21.18	26.44	5.26	92.47	43.99	61.29	3791.12
2	21.19	26.15	4.97	81.62	43.65	60.43	3577.23
3	21.19	26.30	5.11	80.34	43.58	59.15	3681.68
4	21.24	27.54	6.30	100.22	51.01	78.98	4562.72
5	21.25	27.48	6.24	100.22	51.11	78.97	4515.00
6	21.25	27.41	6.16	100.22	51.33	78.97	4454.02
7	21.28	27.33	6.05	92.67	47.10	71.40	4375.26
8	21.28	27.05	5.77	92.74	47.03	71.46	4171.29
9	21.27	27.17	5.90	92.65	46.99	71.38	4263.09
10	21.31	26.06	4.76	72.21	41.38	50.91	3424.10
11	21.31	25.95	4.64	72.06	40.95	50.75	3340.65
12	21.31	25.88	4.57	71.93	40.84	50.62	3288.09
13	21.33	24.79	3.45	58.51	36.41	37.28	2471.79
14	21.33	24.88	3.56	58.44	36.32	37.11	2538.37
15	21.33	24.77	3.44	58.45	36.26	37.12	2454.83
16	21.39	23.80	2.41	48.57	32.07	27.19	1697.40
17	21.39	23.73	2.34	48.97	32.08	27.58	1642.78
18	21.39	23.73	2.34	48.52	31.99	27.23	1639.71
19	21.40	22.99	1.59	42.10	29.06	20.70	1092.89
20	21.39	23.03	1.64	42.02	29.07	20.62	1125.11
21	21.40	23.04	1.55	42.28	29.22	20.88	1133.60
22	21.41	24.68	3.27	57.00	35.94	35.59	2327.39
23	21.41	24.49	3.08	57.43	36.10	36.02	2186.27
24	21.41	24.66	3.24	57.62	36.14	36.21	2307.99
25	21.44	25.74	4.29	69.07	40.50	47.63	3082.19
26	21.44	25.46	4.01	68.15	40.45	47.70	2875.96
27	21.43	25.75	4.31	69.05	40.43	47.62	3097.39

NOTE: Above analysis was performed for data in file H16FP_1

TABLE C.8

Results of Helical 16-Fin Condenser at 1400 rpm

Month, date and time: 11:21:10:59:43
Rotor speed = 1400
Rotameter reading = 40.0

Data Set #	Tci (C)	Tco (C)	Dcw (C)	Ts (C)	Tw (C)	Dmax (C)	Q (W)
1	21.44	23.10	1.67	38.79	29.40	17.35	1022.99
2	21.44	23.11	1.67	38.79	29.40	17.35	1023.59
3	21.44	24.05	2.61	46.29	33.22	24.85	1719.39
4	21.45	24.00	2.56	46.31	32.93	24.86	1678.73
5	21.45	24.03	2.58	46.32	33.16	24.87	1696.93
6	21.46	25.28	3.81	56.46	37.81	35.00	2606.34
7	21.47	25.24	3.77	56.58	37.96	35.11	2574.79
8	21.47	25.23	3.76	56.25	37.85	34.78	2569.39
9	21.48	26.82	5.34	68.82	43.76	47.34	3729.47
10	21.48	26.83	5.36	68.79	43.77	47.31	3740.94
11	21.47	26.75	5.28	68.80	43.76	47.32	3685.49
12	21.49	28.52	7.03	83.70	50.38	62.21	4974.59
13	21.49	28.48	6.99	83.83	50.51	62.34	4946.35
14	21.50	28.53	7.03	83.81	50.34	62.31	4973.88
15	21.50	29.21	7.72	90.23	52.50	68.73	5481.07
16	21.49	26.14	4.65	62.47	40.75	40.98	3219.08
17	21.49	26.03	4.54	62.46	40.65	40.97	3139.91
18	21.49	26.03	4.54	62.36	40.64	40.87	3141.81
19	21.49	27.75	6.25	77.42	47.57	55.93	4402.34
20	21.50	27.77	6.28	77.47	47.57	55.98	4420.37
21	21.50	27.82	6.33	77.54	47.61	56.04	4456.53
22	21.48	24.85	3.36	53.19	36.14	31.71	2274.51
23	21.49	24.86	3.37	53.25	36.38	31.77	2278.69
24	21.49	24.82	3.33	53.37	36.29	31.88	2250.85

NOTE: Above analysis was performed for data in file H16FF_2

TABLE C.9

Results of Helical 16 Fin Condenser at 2800 rpm

Month. date and time: 11:21:11:02:12
Rotor speed = 2800
Rotameter reading = 40.0

Data Set #	Tci (C)	Tco (C)	Dcw (C)	Ts (C)	Tw (C)	Dmax (C)	Q (W)
1	21.43	23.21	1.78	37.28	30.02	15.85	1028.22
2	21.43	23.18	1.75	37.26	30.00	15.82	1008.18
3	21.43	23.18	1.75	37.35	30.06	15.92	1004.56
4	21.42	24.07	2.65	42.71	33.02	21.29	1669.46
5	21.41	24.10	2.69	42.73	32.98	21.32	1702.94
6	21.41	24.06	2.65	42.72	32.97	21.31	1670.76
7	21.37	25.33	3.96	51.45	37.60	30.08	2638.90
8	21.37	25.34	3.97	51.59	37.62	30.23	2641.96
9	21.37	25.36	3.99	51.63	37.93	30.26	2660.08
10	21.39	27.00	5.61	61.69	43.48	40.30	3848.71
11	21.39	27.04	5.65	61.54	43.29	40.15	3877.14
12	21.39	27.01	5.62	61.51	43.36	40.12	3858.40
13	21.45	28.92	7.47	73.43	49.23	51.98	5220.95
14	21.45	28.87	7.42	73.33	49.26	51.88	5180.00
15	21.45	28.83	7.38	73.25	49.32	51.80	5153.57
16	21.46	29.30	7.84	77.68	51.50	56.21	5493.81
17	21.46	29.68	8.22	79.19	52.33	57.73	5772.10
18	21.44	28.23	6.79	68.70	46.79	47.26	4719.09
19	21.46	28.19	6.73	68.37	46.62	46.92	4677.32
20	21.46	28.26	6.80	68.99	47.00	47.53	4727.27
21	21.43	26.09	4.66	55.36	39.76	33.93	3152.15
22	21.43	26.08	4.65	55.39	39.73	33.96	3147.29
23	21.41	26.06	4.65	55.38	39.73	33.97	3143.90
24	21.44	24.68	3.24	46.04	34.44	24.61	2105.56
25	21.44	24.71	3.28	45.86	34.41	24.43	2134.03
26	21.45	24.71	3.27	46.06	34.45	24.61	2126.66

NOTE: Above analysis was performed for data in file H16FP_3

TABLE C.10

Results of Helical 14 Fin Condenser at 700 rpm

Month, date and time: 11:21:10:08:33
Rotor speed = 700
Rotameter reading = 43.0

Data Set #	Tci (C)	Tco (C)	Dcw (C)	Ts (C)	Tw (C)	Dmax (C)	Q (W)
1	21.38	22.18	.79	33.41	25.37	12.02	547.14
2	21.38	22.12	.74	32.67	25.11	11.29	502.83
3	21.38	22.12	.75	32.97	25.17	11.59	509.39
4	21.39	23.01	1.62	43.22	29.29	21.83	1259.56
5	21.38	23.08	1.70	43.30	29.19	21.91	1319.48
6	21.40	23.12	1.72	43.47	29.35	22.08	1340.45
7	21.40	23.93	2.53	52.17	32.98	30.77	1959.71
8	21.40	23.96	2.56	51.85	33.00	30.45	1983.65
9	21.41	23.93	2.53	52.04	32.92	30.64	1959.69
10	21.39	24.78	3.38	61.63	36.96	40.24	2410.54
11	21.41	24.67	3.26	61.56	36.94	40.15	2320.78
12	21.41	24.77	3.36	61.62	36.82	40.21	2394.61
13	21.46	26.27	4.82	72.78	41.57	51.32	3552.44
14	21.45	26.10	4.65	72.81	41.60	51.36	3428.84
15	21.45	26.10	4.65	72.95	41.68	51.49	3385.01
16	21.48	27.20	5.72	91.54	46.32	70.06	4336.15
17	21.48	27.23	5.76	91.10	46.28	69.62	4365.87
18	21.48	27.15	5.67	91.57	47.03	70.08	4195.61
19	21.52	26.79	5.27	92.24	46.30	70.72	3895.43
20	21.52	26.69	5.16	92.32	46.34	70.79	3860.87
21	21.53	26.77	5.24	92.01	46.15	70.48	3966.10
22	21.51	25.68	4.17	67.66	39.50	46.15	3098.58
23	21.50	25.77	4.28	67.48	39.50	45.98	3238.38
24	21.50	25.64	4.14	67.36	39.39	45.86	3119.26
25	21.53	24.31	2.78	53.80	34.04	32.26	2064.40
26	21.53	24.24	2.70	53.85	33.79	32.32	2007.87
27	21.52	24.26	2.74	54.40	33.83	32.88	2031.46
28	21.54	22.65	1.11	38.01	25.83	16.48	779.08
29	21.53	22.64	1.11	38.13	26.76	16.60	778.49
30	21.53	22.64	1.11	38.07	26.73	16.54	779.76

NOTE: Above analysis was performed for data in file H14FP_1

TABLE C.11

Results of Helical 14 Fin Condenser at 1400 rpm

Month, date and time: 11:21:10:23:14
Rotor speed = 1400
Rotameter reading = 42.0

Data Set #	Tci (C)	Tco (C)	Dcw (C)	Ts (C)	Tw (C)	Dmax (C)	Q (W)
1	21.52	22.58	1.05	31.63	26.14	10.10	609.04
2	21.53	22.58	1.05	31.66	26.20	10.13	605.82
3	21.48	23.70	2.21	41.69	30.64	20.21	1505.33
4	21.51	23.68	2.18	41.62	30.60	20.11	1475.86
5	21.52	23.70	2.18	41.76	30.59	20.24	1478.32
6	21.44	24.90	3.46	52.10	35.29	30.66	2466.72
7	21.42	24.85	3.44	51.68	35.43	30.26	2451.16
8	21.43	24.85	3.42	51.86	35.22	30.43	2437.71
9	21.43	25.50	4.07	57.23	37.66	35.80	2939.35
10	21.44	25.65	4.21	56.95	38.06	35.51	3047.02
11	21.46	25.55	4.09	57.08	37.71	35.62	2958.06
12	21.52	27.22	5.70	70.97	43.92	49.45	4197.36
13	21.56	27.30	5.74	71.04	44.01	49.47	4229.64
14	21.54	27.25	5.71	71.11	43.90	49.57	4204.70
15	21.56	28.33	6.77	79.91	47.70	58.34	5021.05
16	21.57	28.35	6.78	79.93	47.83	58.37	5031.74
17	21.57	28.37	6.80	79.99	47.87	58.41	5044.23
18	21.50	26.34	4.84	62.94	40.57	41.44	3532.12
19	21.50	26.31	4.81	63.12	40.48	41.63	3511.86
20	21.51	26.42	4.90	63.30	40.58	41.78	3582.58
21	21.56	24.71	3.15	50.12	34.37	28.56	2198.27
22	21.58	24.68	3.10	50.16	34.26	28.58	2159.74
23	21.56	24.68	3.12	50.11	34.30	28.55	2180.74
24	21.60	23.20	1.59	37.50	28.72	15.90	1011.86

NOTE: Above analysis was performed for data in file H14FP_2C

TABLE C.12

Results of Helical 14-Fin Condenser at 2800 rpm

Month, date and time: 11:21:10:13:35
Rotor speed = 2800
Rotameter reading = 41.0

Data Set #	Tci (C)	Tco (C)	Dcw (C)	Ts (C)	Tw (C)	Dmax (C)	Q (W)
1	21.53	23.16	1.63	34.55	28.03	13.12	947.67
2	21.52	23.17	1.64	34.59	28.05	13.06	958.30
3	21.52	23.21	1.69	34.61	28.02	13.10	996.27
4	21.28	24.03	2.75	41.57	31.45	20.29	1796.15
5	21.30	23.97	2.67	41.55	31.44	20.26	1735.10
6	21.30	24.05	2.75	41.58	31.44	20.28	1791.59
7	21.51	25.50	3.99	48.53	35.42	27.01	2728.71
8	21.52	25.26	3.74	48.97	35.21	27.45	2538.46
9	21.47	25.23	3.77	48.73	35.30	27.26	2561.35
10	21.48	26.37	4.89	56.48	39.38	35.00	3407.45
11	21.47	26.35	4.88	56.93	39.59	35.46	3399.54
12	21.51	26.25	4.74	56.56	39.46	35.05	3296.36
13	21.60	27.92	6.32	65.70	44.07	44.10	4486.17
14	21.59	27.81	6.22	65.80	44.13	44.21	4408.57
15	21.61	27.91	6.30	65.96	44.18	44.35	4469.97
16	21.61	29.48	7.87	76.23	49.44	54.63	5654.60
17	21.62	29.25	7.63	76.32	49.60	54.70	5470.24
18	21.63	29.46	7.83	76.41	49.56	54.78	5625.34
19	21.45	27.45	6.00	62.56	42.28	41.11	4245.23
20	21.48	27.25	5.76	62.49	42.24	41.01	4066.89
21	21.45	27.29	5.84	62.43	42.16	40.98	4120.43
22	21.30	24.42	3.12	45.07	33.20	23.78	2074.61
23	21.32	24.56	3.24	45.11	33.31	23.79	2160.55
24	21.31	24.47	3.16	44.93	33.13	23.63	2103.05
25	21.71	23.16	1.45	34.81	27.94	13.10	786.17
26	21.75	23.26	1.51	34.83	27.96	13.08	860.74
27	21.66	23.27	1.61	34.86	27.98	13.20	932.94

NOTE: Above analysis was performed for data in file H14FP_3

TABLE C.13

Results of Helical 36 Fin Condenser at 700 rpm

Month, date and time: 10:20:16:33:43
Rotor speed = 700
Rotameter reading = 40.5

Data Set #	Tci (C)	Tco (C)	Dcw (C)	Ts (C)	Tw (C)	Dmax (C)	Q (W)
1	20.15	21.36	1.21	34.69	25.88	14.54	823.50
2	20.17	21.43	1.26	34.82	25.92	14.65	859.06
3	20.18	21.32	1.14	34.77	25.96	14.59	772.10
4	20.23	22.57	2.34	47.61	30.88	27.38	1644.98
5	20.23	22.26	2.03	47.82	31.04	27.59	1416.40
6	20.22	22.42	2.21	47.78	31.27	27.56	1546.00
7	20.30	23.20	2.90	59.94	35.24	39.63	2059.17
8	20.31	23.46	3.15	59.97	34.93	39.66	2241.21
9	20.31	23.12	2.81	60.03	34.81	39.72	1988.03
10	20.34	24.55	4.21	68.55	39.00	48.21	3020.64
11	20.36	24.32	3.95	68.59	39.00	48.22	2830.69
12	20.37	24.52	4.15	68.62	38.92	48.25	2976.65
13	20.40	23.69	3.29	66.02	36.30	45.62	2345.22
14	20.40	23.63	3.23	65.98	36.40	45.58	2299.15
15	20.40	23.79	3.39	66.03	36.17	45.63	2419.21
16	20.42	22.95	2.53	56.09	33.83	35.67	1785.97
17	20.42	23.03	2.62	55.93	33.75	35.52	1848.55
18	20.42	22.97	2.55	55.96	33.82	35.54	1798.09
19	20.42	22.34	1.92	40.87	28.89	20.45	1333.22
20	20.43	22.10	1.67	40.79	28.64	20.37	1150.71
21	20.41	22.12	1.71	40.59	28.72	20.18	1179.47
22	20.41	21.83	1.42	34.09	26.27	13.68	964.65
23	20.43	21.72	1.29	34.18	26.24	13.75	866.54
24	20.41	21.73	1.32	34.08	26.36	13.67	894.70

NOTE: Above analysis was performed for data in file -36FP_1

TABLE C.14

Results of Helical 36-Fin Condenser at 1400 rpm

Month. date and time: 10:20:16:39:58
Rotor speed = 1400
Rotameter reading = 40.0

Data Set #	Tci (C)	Tco (C)	Dcw (C)	Ts (C)	Tw (C)	Dmax (C)	Q (W)
1	20.41	21.81	1.40	31.46	26.04	11.05	827.06
2	20.44	21.77	1.33	31.33	26.07	10.88	778.15
3	20.44	21.80	1.36	31.17	26.10	10.73	795.18
4	20.45	22.90	2.45	41.32	30.90	20.86	1601.30
5	20.45	22.80	2.35	41.39	30.78	20.94	1530.27
6	20.45	22.85	2.40	41.30	30.69	20.85	1567.93
7	20.44	24.00	3.55	52.26	36.04	31.82	2414.64
8	20.44	23.87	3.43	52.30	35.91	31.86	2321.88
9	20.42	23.72	3.30	52.21	36.05	31.79	2227.51
10	20.43	24.92	4.49	64.22	41.60	43.79	3105.54
11	20.46	25.47	5.02	64.36	41.66	43.91	3492.50
12	20.45	25.16	4.71	64.57	41.56	44.12	3268.77
13	20.44	26.43	5.99	68.74	45.66	48.30	4208.36
14	20.46	26.23	5.77	68.89	45.72	48.43	4047.98
15	20.47	26.67	6.20	68.93	45.54	48.47	4365.67
16	20.46	24.98	4.53	61.55	40.83	41.10	3133.05
17	20.46	25.21	4.75	61.44	40.71	40.98	3297.64
18	20.47	25.50	5.03	61.47	40.67	41.01	3505.08
19	20.47	24.92	4.45	61.27	40.51	40.80	3078.39
20	20.48	23.60	3.12	48.25	34.30	27.77	2098.22
21	20.51	23.42	2.91	48.36	34.40	27.85	1941.98
22	20.47	23.47	3.00	48.29	34.28	27.81	2006.05
23	20.51	22.38	1.87	35.10	27.84	14.60	1177.25
24	20.47	22.32	1.85	35.11	27.83	14.64	1158.71
25	20.49	22.33	1.84	35.02	27.86	14.53	1153.65

NOTE: Above analysis was performed for data in file H36FP_2

TABLE C.15

Results of Helical 36 Fin Condenser at 2800 rpm

Month. date and time: 10:20:16:43:43
Rotor speed = 2800
Rotameter reading = 40.0

Data Set #	Tci (C)	Tco (C)	Dcw (C)	Ts (C)	Tw (C)	Dmax (C)	Q (W)
1	20.50	22.05	1.55	29.80	26.52	9.30	857.87
2	20.53	21.88	1.35	29.79	26.48	9.26	716.51
3	20.51	22.26	1.74	29.78	26.46	9.27	1003.73
4	20.52	22.92	2.39	34.91	29.71	14.39	1480.71
5	20.52	23.29	2.76	34.92	29.72	14.39	1755.82
6	20.51	22.80	2.29	35.03	29.91	14.52	1402.44
7	20.51	24.06	3.55	42.99	34.43	22.48	2337.12
8	20.51	23.84	3.33	43.21	34.20	22.70	2169.10
9	20.49	24.22	3.73	42.41	34.32	21.92	2465.21
10	20.52	25.67	5.15	51.24	39.73	30.73	3511.70
11	20.51	25.71	5.19	51.05	39.68	30.54	3544.39
12	20.49	25.81	5.32	51.16	39.85	30.67	3637.20
13	20.54	27.73	7.20	62.05	46.19	41.51	5019.56
14	20.51	27.71	7.20	61.94	46.25	41.43	5022.39
15	20.50	27.76	7.26	62.14	46.28	41.65	5067.25
16	20.42	25.18	4.76	48.00	37.72	27.58	3227.41
17	20.43	25.18	4.75	48.02	37.81	27.59	3215.78
18	20.41	25.24	4.83	48.13	37.59	27.72	3277.74
19	20.41	25.24	4.83	48.58	38.33	28.17	3277.19
20	20.41	25.14	4.74	48.51	38.19	28.10	3209.41
21	20.35	25.42	5.07	49.93	38.99	29.57	3452.12
22	20.37	25.27	4.90	49.86	38.69	29.49	3325.45
23	20.37	25.33	4.96	49.89	38.93	29.52	3375.67
24	20.42	27.05	6.63	57.73	43.99	37.31	4601.58
25	20.37	26.92	6.55	57.74	43.75	37.37	4543.17
26	20.38	27.04	6.66	57.53	43.74	37.15	4622.10
27	20.43	22.50	2.07	31.69	27.45	11.26	1240.32
28	20.46	22.40	1.95	31.62	27.37	11.17	1152.56
29	20.46	22.42	1.96	31.64	27.34	11.18	1165.32

NOTE: Above analysis was performed for data in file H36FP_3

LIST OF REFERENCES

1. Daley, T. J., The Experimental Design and Operation of a Wickless Heat Pipe, M. S. Thesis, Naval Postgraduate School, Monterey, California, June 1970.

2. Newton, W. H., Performance Characteristic of Rotating Non-capillary Heat Pipes, M. S. Thesis, Naval Postgraduate School, Monterey, California, June 1971.

3. Woodard, J. S., The Operation of Rotating Non-capillary Heat Pipes, M. S. Thesis, Naval Postgraduate School, Monterey, California, March 1972.

4. Schafer, C. E., Augmenting the Heat Transfer Performance of Rotating, Two-Phase Thermosyphons, M. S. Thesis, Naval Postgraduate School, Monterey, California, September 1974.

5. Tucker, J. L., Design Improvements on a Rotating Heat Pipe Apparatus, M. S. Thesis, Naval Postgraduate School, Monterey, California, September 1976.

6. Loynes, J. L., Design Improvements on a Rotating Heat Pipe Apparatus, M. S. Thesis, Naval Postgraduate School, Monterey, California, September 1976.

7. Wagenseil, L. L., Heat Transfer Performance of Rotating Heat Pipes, M. S. Thesis, Naval Postgraduate School, Monterey, California, September 1976.

8. Tantrakul, C., Condensation Heat Transfer Inside Rotating Heat Pipes, M. S. and Engineer's Theses, Naval Postgraduate School, Monterey, California, June 1977.

9. Weigel, H. J., Heat Transfer Performance of a Rotating Heat Pipe Using Different Condensers and Working Fluids, M. S. Thesis, Naval Postgraduate School, Monterey, California, June 1979.

10. Gardner, G. H., An Experimental Evaluation of the Thermal Performance of a Rotating Heat Pipe with Internal Axial Fins, M. S. Thesis, Naval Postgraduate School, Monterey, California, June 1983.

11. Leppert, G., and Nimmo, B., "Laminar Film Condensation on Surfaces Normal to Body or Internal Forces," Transactions of the ASME, p. 178, February 1968.

12. Nimmo, B. G., and Leppert, G., "Laminar Film Condensation on Finite Horizontal Surface," Clarckson College of Technology, Dotsdam, New York, 1970.

13. Roetzel, W., and Neuman, M., "Uniform Heat Flux in a Paper Drying Drum with a Non-Cylindrical Condensation Surface Operating Under Rimming Conditions," Council for Scientific and Industrial Research, Pretoria, South Africa, March 1974.

14. Nicol, A. A., and Gacesa, M., "Condensation of Steam on a Rotating Vertical Cylinder," ASME Paper No. 69-HT-36. (1969)

15. Kline, S. J., and McClintock, F. A., "Describing Uncertainties in Single Sample Experiments," Mechanical Engineering p.3, January 1953.

INITIAL DISTRIBUTION LIST

		No. Copies
1.	Defense Technical Information Center Cameron Station Alexandria, Virginia 22314	2
2.	Library, Code 0142 Naval Postgraduate School Monterey, California 93943	2
3.	Department Chairman, Code 69 Department of Mechanical Engineering Naval Postgraduate School Monterey, California 93943	1
4.	Professor P. J. Marto, Code 69Mx Department of Mechanical Engineering Naval Postgraduate School Monterey, California 93943	5
5.	Dr. A. S. Wanniarachchi, Code 69 Department of Mechanical Engineering Naval Postgraduate School Monterey, California 93943	1
6.	Dz. K. Komutanliği Okullar ve Kurslar Dairesi Bakanliklar, Ankara, Turkey	5
7.	Deniz Harp Okulu Kütüphanesi Heybeliada, İstanbul Turkey	1
8.	İstanbul Teknik Üniversitiesi Kütüphanesi İstanbul, Turkey	1
9.	Boğazici Üniversitesi Kütüphanesi Istanbul, Turkey	1

10. Orta Doğu Teknik Universitesi Kütüphanesi
Ankara, Turkey — 1

11. Adnan Nefesoğlu
Attar Sokak 15/11
Gazi Osman Paşa
Ankara, Turkey — 3

207206

Thesis
N3543
c.1

Nefesoglu
Heat transfer measurement of internally finned rotating heat pipes.

207206

Thesis
N3543
c.1

Nefesoglu
Heat transfer measurement of internally finned rotating heat pipes.

thesN3543
Heat transfer measurements of internally
3 2768 002 01781 6
DUDLEY KNOX LIBRARY